PERGAMON

International Journal of Solids and Structures 37 (2000) 4211–4238

INTERNATIONAL JOURNAL OF SOLIDS and STRUCTURES

www.elsevier.com/locate/ijsolstr

Internal residual stresses in elastically homogeneous solids: II. Stress fluctuations near a crack tip and effective energy release rate

V.A. Buryachenko*, [1]

Air Force Research Laboratory, Materials Directorate, AFRL/MLBC, Bldg. 654, Wright–Patterson AFB, OH 45433-7750, USA

Received 16 June 1998; in revised form 14 December 1998

Abstract

We consider a linearly elastic composite medium which consists of an homogeneous matrix containing a crack and a homogeneous and statistically uniform random set of ellipsoidal inclusions; the elastic properties of the matrix and the inclusions are the same, but the stress-free strains fluctuate. We obtain the estimation of both the statistical average and the conditional average of stress intensity factors. The relations for the second statistical moments of stresses in the vicinity of the crack tip, averaged over the ensemble realization, are proposed as well. A method for construction of the effective strength surface of matrix composites, according to the properties of their components is developed. The expression for effective energy release rate is also derived. The fracture probabilities of separate components are calculated.

Keywords: Ceramics; Thermoelastic; Crack; Energy release rate; Micro-mechanics; Green function; Homogenization

1. Introduction

In ceramic materials a common source of internal stresses is the thermal expansion anisotropy (Al_2O_3) or the thermal mismatch (Si–Si_3N_4) in the components, as well as a phase transformations (ZrO_2). In some cases (for example during cooling from the fabrication temperature), residual stresses are large enough to produce microcracking along grain boundaries or macrocrack propagation (Cutler and Vircar, 1985; Luo and Stevens, 1993). The strength calculations of the composites serve as examples of a nonlinear problem. Although significant advancement has been archived with respect to disorder and

* Fax.: +001-937-656-7429.

E-mail address: buryach@aol.com (V.A. Buryachenko).

[1] Permanent address: Department of Mathematics, Moscow State University of Engineering Ecology, 107884 Moscow, Russia.

0020-7683/00/$ - see front matter
PII: S0020-7683(99)00125-0

nonlinearity separately, the situation becomes quite complex and interesting when both are important. Since the widely used Mori–Tanaka method of average deformation allows one to estimate only average stresses in components (see, for references, Buryachenko, 1996), it is evident that they are used for linearization of functions describing nonlinear effects, such as strength (Arsenault and Taya, 1987; Reifsnider and Gao, 1991). This can lead to qualitatively wrong conclusions, because of significant inhomogeneity of the stress field in the components (especially in the matrix), which will be shown in the present paper by an example of a composite with isotropic components.

The exact solution is possible for deterministic structure by means of numerical methods. Composites with regular structure (Evans, 1987, 1989; Fu and Evans, 1985; Tvergard and Hutchinson, 1988) and modifications of self-consistent scheme models (Laws and Lee, 1989) among them are only two-dimensional and, often the elastic anisotropy is neglected. Although these regularization theories allow detailed stress calculations (for instance local stress intensity factors for flaws in the real interface can be derived), they do not seem suited to describe the real three-dimensional and stochastic microstructure of polycrystals.

A significant advance has been made in the study of residual stresses by the Monte-Carlo method of numerical simulation of the random structure of materials (Ortiz and Suresh, 1993; Nakamura and Suresh, 1993). Because of the long computing time, two-dimensional models of composites with a special random structure are used. The numerical simulation points to the fact that the spatial distribution of components has a significant effect on the local stresses. Therefore, these methods do not seem suited to predicting the strength of three-dimensional random structures.

Another direction of residual stress research is directly related to the derived exact relation for second statistical moment of stress averaged over volume of the composite of some special structure if one neglects the nonhomogeneity of elastic constants (see for references Buryachenko, 1999b). This second stress moment is given the name covariance matrix by Ortiz and Molinari (1988). They assumed that the residual stresses at each point are normally distributed and used a standard method of calculation of microcrack formation under random loading.

The study of macrocrack propagation in composite materials is of immediate interest to industry. The problem of interaction between a crack tip and a source of internal stress (which is given an Eshelby transformation of its stress-free state) is discussed by a number authors (see, for references, e.g. Rice and Pohanka, 1979; Stump and Budiansky, 1989; Rice, 1985). A considerable number of papers are concerned with a study of crack-microcracks or crack-microinclusions interactions (appropriate, but by no means exhaustive, references are provided by the review of Kachanov, 1993; see also Cutler and Vircar, 1985; Taya et al., 1990; Chudnovsky and Wu, 1993; Nemat-Nasser and Hori, 1993; Bover and Ortiz, 1993). As this takes place, a variety of simplification are used: two-dimensional problem, regular structure of the microdefect field, approximation of microcrack array by a 'soft inclusion', weak interaction between microinclusions, numerical simulation of inclusion distribution with subsequent solution of the determinate problem.

Previous analyses in fracture mechanics have not usually focused on the influence of the statistical effects of residual stresses. But it becomes obvious that, because of random residual stresses, the energy release rate at a tip of crack is also random. With the simplifying assumption of an elastically homogeneous plane with a macrocrack, the random finite set of inclusions is modeled as an elastic continuum within which the deterministic stress-free transformation has a magnitude equal to a statistical average of the random transformed field (McMeeking and Evans, 1982; Budiansky et al., 1983; Lambropoulos, 1986). Taking into account the stochastic nature of the problem being analyzed and Monte Carlo simulation, Lipetzky and Kreher (1994) considered a two-dimensional problem with a macrocrack inside the random field of residual stresses.

In the present paper, we consider a linearly elastic composite medium, which consists of a homogeneous matrix containing a crack and a homogeneous and statistically uniform random set of

ellipsoidal inclusions; elastic properties of matrix and the inclusions are the same, but stress-free strains fluctuate. We obtain the estimation of both the average and conditional average of stress intensity factors. We show that, at least for an infinite statistically homogeneous field of transforming inclusions, the proposed method leads to a valid result (average stress intensity factor equals zero), which cannot be applied for practical purposes. The relations for statistical second moments of stresses in the vicinity of crack tip averaged over ensemble realization are proposed as well. We show a fundamental difference between the estimations of statistical moments of stresses for an infinite inclusion field and for an arbitrary large (but finite) inclusion cloud. The case of regular structure of the inclusions is discussed as well.

Of course the composite can be considered as a medium with an infinite number of randomly located elements under random loading of each one. In this case the problem of fracture calculations becomes rather complicated although phenomenological methods of its approximate solution are well known (see Bolotin, 1993; Sobczuk and Spencer, 1991), and will not be pursued in this paper. In the present paper, a simple method of strength and fracture calculations is proposed which can be employed in the micromechanics of composites and is based on the use of a random character of stresses within components. As an example of this method one shows the influence of random character of residual stresses on the probability of fracture of composites.

2. Interaction of the crack and inclusion in an infinite matrix

Let us consider a penny-shaped crack with radius R^{c}, center $\mathbf{x}^{\mathrm{c}}=(0, 0, 0)$ and unit normal $\mathbf{n}=(1, 0, 0)$ to the crack surface S in an infinite elastic body. It is well known that the problem of a linear elastic solid with a crack under remote loading $\boldsymbol{\sigma}(\mathbf{x})$ has the same stress intensity factors as the problem with the crack faces loaded by traction $\mathbf{t}(\mathbf{s})=-\mathbf{n}(\mathbf{s})\boldsymbol{\sigma}(\mathbf{s})$ $(\mathbf{s}\in S)$ and stresses vanishing at infinity. This loading generates a singular stress components $\boldsymbol{\sigma}$ ahead of the crack tip $\mathbf{z}\in\Gamma^{\mathrm{c}}$

$$\boldsymbol{\sigma}(\mathbf{x})\sim\mathbf{J}(\theta, \mathbf{z})/\sqrt{\rho}, \tag{1}$$

where $\rho\equiv\min_{\mathbf{s}\in\Gamma^{\mathrm{c}}}|\mathbf{x}-\mathbf{s}|$ is a minimum distance between $\mathbf{x}$ and crack tip Γ^{c}, $\mathbf{z}\equiv\arg\min_{\mathbf{s}\in\Gamma^{\mathrm{c}}}|\mathbf{x}-\mathbf{s}|$; (ρ, θ) are the polar coordinates of the point $\mathbf{x}$ with the origin of the polar coordinates located at the point $\mathbf{z}$. $\mathbf{J}(\theta, \mathbf{z})$ is a tensor stress intensity factor, which is connected with the usual stress intensity factors (SIF) $\mathbf{K}(\mathbf{z})$

$$K_j(\mathbf{z})=J_{1j}(0, \mathbf{z})\sqrt{2\pi},\ (j=1, 2, 3). \tag{2}$$

In so doing, the axes of the local system are labeled to agree with mode number designations for stress intensity factors K_j $(j=1, 2, 3)$ (see Rice, 1989) and $\mathbf{K}(\mathbf{z})=(K_1(\mathbf{z}), K_2(\mathbf{z}), K_3(\mathbf{z}))^{\top}\equiv(K_{\mathrm{I}}(\mathbf{z}), K_{\mathrm{II}}(\mathbf{z}), K_{\mathrm{III}}(\mathbf{z}))^{\top}$ are defined by the integral

$$\mathbf{K}(\mathbf{z})=\int_S\mathbf{k}(\mathbf{z}, \mathbf{s})\mathbf{t}(\mathbf{s})\mathrm{d}\mathbf{s} \tag{3}$$

over surface $\mathbf{s}\in S$ from the crack-face weight functions $\mathbf{k}(\mathbf{z}, \mathbf{s})$, for which, one may observe that symmetry requires $k_{12}=k_{13}=k_{21}=k_{23}=k_{31}=k_{32}=0$; the tensile mode crack face weight functions, k_{11}, and the shear functions, k_{22} and k_{33}, are given by Rice (1989) and Gao (1988). For simplicit'y sake, with the following calculations, we will formally define $\mathbf{J}(\theta, \mathbf{z})$ in the form of Eq. (3):

$$\mathbf{J}(\theta, \mathbf{z}) = \int_S \mathbf{g}(\theta, \mathbf{z}, \mathbf{s})\mathbf{t}(\mathbf{s})d\mathbf{s}, \tag{4}$$

where $\mathbf{g}(\theta, \mathbf{z}, \mathbf{s})$ is called of as tensor crack-face weight vector-function. By virtue of the fact that in linear fracture mechanics, usually only the SIF Eq. (3) plays an important role, it is not necessary to know all components of the third rank tensor, $\mathbf{g}(\theta, \mathbf{z}, \mathbf{s})$, which do not coincide with the corresponding components of $\mathbf{k}(\mathbf{z}, \mathbf{s})$ Eq. (3).

For a penny-shaped crack in an isotropic medium, the relations of $\mathbf{K}(\mathbf{z})$ Eq. (3) may be significantly simplified. We will use the solution by Fabrikant (1989), who showed that the representation Eq. (3) can actually be expressed in the convenient complex form. Kachanov and Laures (1989) eliminated the singularities in the proposed integrals by way of transfer to the new coordinate system; these representations are shown in Appendix A with the corrections of some misprints.

Let us consider an infinite medium containing a crack S and an inclusion v_i with stress-free transformation jump $\boldsymbol{\beta}_1(\mathbf{x})$, $\mathbf{x} \in v_i$ under remote loading by the homogeneous stress field, $\boldsymbol{\sigma}^0 \equiv \text{const}$. Then the remote loading and the inclusion effect on a crack may be replaced by means of a traction $\mathbf{t}(\mathbf{s})$ on a crack surface $\mathbf{s} \in S$,

$$\mathbf{t}(\mathbf{s}) = -\mathbf{n}(\mathbf{s})\left[\boldsymbol{\sigma}^0 + \int \boldsymbol{\Gamma}(\mathbf{s}-\mathbf{x})\boldsymbol{\beta}_1(\mathbf{x})d\mathbf{x}\right], \tag{5}$$

where the integral operator kernel, $\boldsymbol{\Gamma}(\mathbf{x}-\mathbf{y}) \equiv -\mathbf{L}[\mathbf{I}\delta(\mathbf{x}-\mathbf{y}) + \nabla\nabla\mathbf{G}(\mathbf{x}-\mathbf{y})\mathbf{L}]$, is defined by the infinite-homogeneous-body Green's tensor $\mathbf{G}$ of the Lamé equation of an homogeneous medium with elastic modulus tensor $\mathbf{L}$. Hereafter, the integration in the volume integrals are carried out over the whole space.

The Eq. (5) can be rewritten in more compact form

$$\mathbf{t}(\mathbf{s}) = \mathbf{t}(\mathbf{s}, v_i, \mathbf{x}_i) = -\mathbf{n}(s)\left[\boldsymbol{\sigma}^0 + \mathbf{T}_i(\mathbf{s}-\mathbf{x}_i, \boldsymbol{\beta}_1)\bar{v}_i\right], \tag{6}$$

$$\mathbf{T}_i(\mathbf{x}-\mathbf{x}_i, \boldsymbol{\beta}_1) = \bar{v}_i^{-1}\int \boldsymbol{\Gamma}(\mathbf{x}-\mathbf{y})\boldsymbol{\beta}_1(\mathbf{y})V_i(\mathbf{y})d\mathbf{y}. \tag{7}$$

For $\mathbf{x} \in v_i$ we will use additional notation:

$$\mathbf{Q}_i(\mathbf{x}, \boldsymbol{\beta}_1) \equiv -\mathbf{T}_i(\mathbf{x}-\mathbf{x}_i, \boldsymbol{\beta}_1)\bar{v}_i = -\int \boldsymbol{\Gamma}(\mathbf{x}-\mathbf{y})\boldsymbol{\beta}_1(\mathbf{y})V_i(\mathbf{y})d\mathbf{y}, \mathbf{x} \in v_i, \tag{8}$$

(see Buryachenko, 1999b for details; as well as Buryachenko and Rammerstorfer, 1999).

For the ellipsoidal homogeneous incision $\boldsymbol{\beta}_i(\mathbf{x}) \equiv \boldsymbol{\beta}_1^{(i)} = \text{const.}$, the tensors $\mathbf{Q}_i(\mathbf{x}, \boldsymbol{\beta}_1) = \mathbf{Q}_i\boldsymbol{\beta}_1^{(i)}$, $\mathbf{T}_i(\mathbf{x}-\mathbf{x}_i, \boldsymbol{\beta}_1) = \mathbf{T}_i(\mathbf{x}-\mathbf{x}_i)\boldsymbol{\beta}_1^{(i)}$ are known (see, e.g. Buryachenko and Rammerstorfer, 1997).

After that, the values of the SIF $\mathbf{K}$ and tensor SIF $\mathbf{J}$ produced by both the remote loading and a single inclusion v_i can be estimated by the use of Eqs. (3) and (4):

$$\mathbf{K}(\mathbf{z}, v_i, \mathbf{x}_i) = \mathbf{K}^0(\mathbf{z}) + \mathbf{K}^1(\mathbf{z}, v_i, \mathbf{x}_i), \tag{9}$$

$$\mathbf{J}(\theta, \mathbf{z}, v_i, \mathbf{x}_i) = \mathbf{J}^0(\theta, \mathbf{z}) + \mathbf{J}^1(\theta, \mathbf{z}, v_i, \mathbf{x}_i), \tag{10}$$

respectively, where

$$\mathbf{K}^1(\mathbf{z}, v_i, \mathbf{x}_i) \equiv -\int_S \mathbf{g}(\mathbf{z}, \mathbf{s})\mathbf{n}(s)\mathbf{T}_i(\mathbf{s}-\mathbf{x}_i, \boldsymbol{\beta}_1)d\mathbf{z} \tag{11}$$

$$\mathbf{J}^1(\theta,\ \mathbf{z},\ v_i,\ \mathbf{x}_i) \equiv -\int_S \mathbf{g}(\theta,\ \mathbf{z},\ \mathbf{s})\mathbf{n}(s)\mathbf{T}_i(\mathbf{s}-\mathbf{x}_i,\ \boldsymbol{\beta}_1)\mathrm{d}\mathbf{z}, \tag{12}$$

and the superscript '0' denotes SIFs in the untransformed body ($\boldsymbol{\beta} \equiv \mathbf{0}$) subjected to the given external loading $\boldsymbol{\sigma}^0$. Hereafter, the superscript '1' stands for the residual stress generated SIFs (also called the internal SIFs). $\mathbf{K}^1(\mathbf{z},\ v_i,\ \mathbf{x}_i)$ and $\mathbf{J}^1(\theta,\ \mathbf{z},\ v_i,\ \mathbf{x}_i)$ identify the impact of a single isolated transformed inclusion v_i on the SIF and the tensor SIF, respectively.

3. The average and conditional mean values of SIF for isolated crack in composite material

Let a penny-shaped crack of radius R^{c} with center $\mathbf{x}^{\mathrm{c}}=(0,\ 0,\ 0)$ and unit normal $\mathbf{n}=(1,\ 0,\ 0)$ be located in an elastically homogeneous composite with a statistical homogeneous field of transformed inclusions v_i ($i = 1, 2,...$). In the subsequent presentation, we will make use of the following definition for some functions $\mathbf{f}(\boldsymbol{\sigma},\ \mathbf{t},\ \mathbf{J},\ \mathbf{K})$. The notations, $\mathbf{f}(\mathbf{x}|v_i,\ \mathbf{x}_i)$ and $\mathbf{f}(\mathbf{x}|S,\ v_i,\ \mathbf{x}_i)$, denote the values of the random function $\mathbf{f}$ of the surrounding inclusions at the point $\mathbf{x}$, under the condition that the inclusion, v_i with center $\mathbf{x}_i$, is fixed (in the absence of a crack) and under the condition that the inclusion v_i and the crack S are fixed, respectively. The notations $\langle\mathbf{f}(\mathbf{x})|v_i,\ \mathbf{x}_i\rangle$ and $\langle\mathbf{f}(\mathbf{x})|S,\ v_i,\ \mathbf{x}_i\rangle$ are used for the conditional averages of appropriate random variables taken for the ensemble of a statistically homogeneous ergodic field $X=(v_j)$. An added sign ';' in the conditional average $\langle\mathbf{f}(\mathbf{x})|;v_i,\ \mathbf{x}_i\rangle$ denotes the case $\mathbf{x} \notin v_i$.

The stress field in any point $\mathbf{x}$ is defined by the superposition of the external loading $\boldsymbol{\sigma}^0$ and by the perturbation generated by both the transformed inclusions and by the crack

$$\boldsymbol{\sigma}(\mathbf{x}) = \boldsymbol{\sigma}^0 + \int \boldsymbol{\Gamma}(\mathbf{x}-\mathbf{y})[\boldsymbol{\beta}_1(\mathbf{y}) - \langle\boldsymbol{\beta}_1\rangle]\mathrm{d}\mathbf{y} + \mathbf{J}(\theta,\ \mathbf{z})/\sqrt{\rho}. \tag{13}$$

The expected value of the right-hand-side integral in Eq. (13) over the ensemble realization vanishes

$$\langle\int \boldsymbol{\Gamma}(\mathbf{x}-\mathbf{y})[\boldsymbol{\beta}_1(\mathbf{y}) - \langle\boldsymbol{\beta}_1\rangle]\mathrm{d}\mathbf{y}\rangle \equiv \mathbf{0}, \tag{14}$$

and the expected value of the tensor $\mathbf{K}$ is defined by Eq. (3),

$$\langle\mathbf{K}(\mathbf{z})\rangle = \int \mathbf{k}(\mathbf{z},\ \mathbf{s})\langle\mathbf{t}(\mathbf{s})\rangle\mathrm{d}\mathbf{s}, \tag{15}$$

where the expected value of the traction $\langle\mathbf{t}(\mathbf{s})\rangle$ may be found by the use of Eq. (14),

$$\langle\mathbf{t}(\mathbf{s})\rangle = -\mathbf{n}(s)\left\{\boldsymbol{\sigma}^0 + \langle\int \boldsymbol{\Gamma}(\mathbf{s}-\mathbf{y})[\boldsymbol{\beta}_1(\mathbf{y}) - \langle\boldsymbol{\beta}_1\rangle]\mathrm{d}\mathbf{y}\rangle\right\} \equiv -\mathbf{n}(s)\boldsymbol{\sigma}^0. \tag{16}$$

Thus the expectation value of SIFs $\mathbf{K}$ coincides with the stress intensity factor $\mathbf{K}^0(\mathbf{z})$ for an isolated crack inside the infinite medium without residual stresses:

$$\langle\mathbf{K}(\mathbf{z})\rangle \equiv \mathbf{K}^0(\mathbf{z}). \tag{17}$$

This result is an exact one and does not depend on the microtopology of statistically homogeneous composites, this is a consequence of a self-equilibrium of internal residual stresses $\langle\boldsymbol{\sigma}\rangle\ (\mathbf{x}) \equiv \boldsymbol{\sigma}^0$. It is obvious that the use of this estimation makes no sense for strength calculation. The applications of Eqs. (15) and (16) do not seem suited to strength calculations because the fracture takes place at a particular point in the vicinity of a crack tip. This point may be located inside either the matrix or in an inclusion.

Therefore, for the fracture analysis of composites, the estimations of conditional averages, either $\langle \mathbf{K}(\mathbf{z})|v_i,\ \mathbf{x}_i\rangle$ or $\langle \mathbf{K}(\mathbf{z})|v_0,\ \mathbf{x}_0\rangle$, under the conditions that either the center of the inclusion v_i or the matrix v_0 are located in the point $\mathbf{x}_i$ or $\mathbf{x}_0$, respectively, are preferred over the average $\langle \mathbf{K}(\mathbf{z})\rangle$.

Let us locate an arbitrary inclusion v_i with the center $\mathbf{x}_i$ alongside the crack. Then the stress field $\boldsymbol{\sigma}(\mathbf{x}|S,\ v_i,\ \mathbf{x}_i)$ in any point $\mathbf{x}$ can be decomposed into

$$\boldsymbol{\sigma}(\mathbf{x}|S,\ v_i,\ \mathbf{x}_i) = \boldsymbol{\sigma}^{\mathrm{ac}}(\mathbf{x}|v_i,\ \mathbf{x}_i) + \mathbf{J}(\theta,\ \mathbf{z}|v_i,\ \mathbf{x}_i)/\sqrt{\rho}, \tag{18}$$

where $\boldsymbol{\sigma}^{\mathrm{ac}}(\mathbf{x}|v_i,\ \mathbf{x}_i)$ and $\mathbf{J}(\theta,\ \mathbf{z}|v_i,\ \mathbf{x}_i)$ are determined by the actions of the inclusions and the remote loading (in the absence of a crack), and by the crack provided that there is a fixed inclusion v_i with the center $\mathbf{x}_i$. The indicated terms may be found by the use of the formulae

$$\boldsymbol{\sigma}^{\mathrm{ac}}(\mathbf{x}|v_i,\ \mathbf{x}_i) = \boldsymbol{\sigma}^0 + \int \boldsymbol{\Gamma}(\mathbf{x}-\mathbf{x}_p)[\boldsymbol{\beta}_1(\mathbf{x}_p)V(\mathbf{x}_p|v_i,\ \mathbf{x}_i) - \langle\boldsymbol{\beta}_1\rangle]\mathrm{d}\mathbf{s}, \tag{19}$$

$$\mathbf{t}(\mathbf{s}|v_i,\ \mathbf{x}_i) = -\mathbf{n}(\mathbf{s})\left\{\boldsymbol{\sigma}^0 + \int \boldsymbol{\Gamma}(\mathbf{s}-\mathbf{x}_p)[\boldsymbol{\beta}_1(\mathbf{x}_p)V(\mathbf{x}_p|v_i,\ \mathbf{x}_i) - \langle\boldsymbol{\beta}_1\rangle]\mathrm{d}\mathbf{s}\right\}, \tag{20}$$

in conjunction with Eq. (4). Here, $V(\mathbf{x}_p|v_i,\ \mathbf{x}_i)$ is a random characteristic function of an argument $\mathbf{x}_p$, under the condition that the inclusion v_i with center $\mathbf{x}_i$ is fixed.

To estimate of conditional average of Eq. (18),

$$\langle\boldsymbol{\sigma}(\mathbf{x}|S,\ v_i,\ \mathbf{x}_i)\rangle = \langle\boldsymbol{\sigma}^{\mathrm{ac}}(\mathbf{x})|v_i,\ \mathbf{x}_i\rangle + \langle\mathbf{J}(\theta,\ \mathbf{z}|v_i,\ \mathbf{x}_i)\rangle/\sqrt{\rho}, \tag{21}$$

over the ensemble realization of the surrounding inclusions, we start with an evaluation of the conditional average $\langle\boldsymbol{\sigma}^{\mathrm{ac}}(\mathbf{x})|v_i,\ \mathbf{x}_i\rangle$.

Averaging Eq. (19) by the use of the conditional probability density $\varphi(v_p,\ \mathbf{x}_p|v_i,\ \mathbf{x}_i) = \delta(\mathbf{x}_p - \mathbf{x}_i) + \varphi(v_p,\ \mathbf{x}_p|;v_i,\ \mathbf{x}_i)$ leads to

$$\langle\boldsymbol{\sigma}^{\mathrm{ac}}(\mathbf{x})|v_i,\ \mathbf{x}_i\rangle = \boldsymbol{\sigma}^0 + \mathbf{T}_i(\mathbf{x}-\mathbf{x}_i,\ \boldsymbol{\beta}_1)\bar{v}_i + \int\left[\mathbf{T}_p(\mathbf{x}-\mathbf{x}_p,\ \boldsymbol{\beta}_1)\bar{v}_p\varphi(v_p,\ \mathbf{x}_p|;v_i,\ \mathbf{x}_i) - \boldsymbol{\Gamma}(\mathbf{x}-\mathbf{x}_p)\langle\boldsymbol{\beta}_1\rangle\right]\mathrm{d}\mathbf{x}_p. \tag{22}$$

Here, it is necessary to recognize two cases of the location $\mathbf{x}$: $\mathbf{x}\in v_i$ and $\mathbf{x}\notin v_i$. Here and below, for formula simplifications, we will use the assumption of a special composite structure (see Eq. 3.14 in Buryachenko, 1999b), which includes the case of statistical isotropy of composites. Then in the first case, when $\mathbf{x}\in v_i$, we obtain

$$\langle\boldsymbol{\sigma}^{\mathrm{ac}}(\mathbf{x})|v_i,\ \mathbf{x}_i\rangle = \boldsymbol{\sigma}^0 + \mathbf{Q}_i\langle\boldsymbol{\beta}_1\rangle - \mathbf{Q}_i(\mathbf{x},\ \boldsymbol{\beta}_1). \tag{23}$$

If the relevant point, $\mathbf{x}$, lies outside the fixed inclusion v_i, Eq. (22) can be used. As can be seen from Eq. (22), the range of the action of surrounding inclusions v_p ($p\neq i$) is localized in the neighborhood of fixed inclusion v_i; that is, the so-called locality principle (see, e.g. Buryachenko and Lipanov, 1986a, 1986b).

We now turn our attention to the analysis of the case when the point considered $\mathbf{x}_0$ is located inside the matrix v_0. Analogously with Eq. (22), we find

$$\langle\boldsymbol{\sigma}^{\mathrm{ac}}(\mathbf{x})|v_0,\ \mathbf{x}_0\rangle = \boldsymbol{\sigma}^0 + \int\left[\mathbf{T}_p(\mathbf{x}-\mathbf{x}_p,\ \boldsymbol{\beta}_1)\bar{v}_p\varphi(v_p,\ \mathbf{x}_p|;v_0,\ \mathbf{x}_0) - \boldsymbol{\Gamma}(\mathbf{x}-\mathbf{x}_p)\langle\boldsymbol{\beta}_1\rangle\right]\mathrm{d}\mathbf{x}_p. \tag{24}$$

In a similar manner, the estimation of the conditional expectation of values $\langle\mathbf{t}(\mathbf{s})|v_i,\ \mathbf{x}_i\rangle$ and $\langle\mathbf{t}(\mathbf{s})|v_0,\ \mathbf{x}_0\rangle$ may be derived:

$$\langle \mathbf{t}(\mathbf{s})|v_i, \mathbf{x}_i\rangle = -\mathbf{n}(\mathbf{s})\Big\{\boldsymbol{\sigma}^0 + \mathbf{T}_i(\mathbf{x}-\mathbf{x}_i, \boldsymbol{\beta}_1)\bar{v}_i + \int\big[\mathbf{T}_i(\mathbf{x}-\mathbf{x}_p, \boldsymbol{\beta}_1)\bar{v}_p\varphi(v_p, \mathbf{x}_p|;v_i, \mathbf{x}_i) - \boldsymbol{\Gamma}(\mathbf{x}-\mathbf{x}_p)\langle\boldsymbol{\beta}_1\rangle\big]\mathrm{d}\mathbf{x}_p\Big\}, \tag{25}$$

$$\langle \mathbf{t}(\mathbf{s})|;v_0, \mathbf{x}_0\rangle = -\mathbf{n}(\mathbf{s})\Big\{\boldsymbol{\sigma}^0 + \int\big[\mathbf{T}_p(\mathbf{x}-\mathbf{x}_p, \boldsymbol{\beta}_1)\bar{v}_p\varphi(v_p, \mathbf{x}_p|;v_0, \mathbf{x}_0) - \boldsymbol{\Gamma}(\mathbf{x}-\mathbf{x}_p)\langle\boldsymbol{\beta}_1\rangle\big]\mathrm{d}\mathbf{x}_p\Big\}. \tag{26}$$

When calculation of the right-hand-side integrals in Eqs. (25) and (26) is carried out, it is necessary to test the possible locations $\mathbf{s}$ with respect to the inclusion v_p: $\mathbf{s}\in v_p$ or $\mathbf{s}\notin v_p$, that can be calculated with ease.

After finding the average conditional tractions on the crack face described by Eqs. (25) and (26), we obtain the final result for the conditional expectation of values of both SIFs and the tensor SIFs:

$$\langle \mathbf{K}(\mathbf{z})|v_J, \mathbf{x}_J\rangle = \int_S \mathbf{k}(\mathbf{z}, \mathbf{s})\langle \mathbf{t}(\mathbf{s})|v_J, \mathbf{x}_J\rangle\mathrm{d}\mathbf{s} \tag{27}$$

$$\langle \mathbf{J}(\theta, \mathbf{z})|v_J, \mathbf{x}_J\rangle = \int_S \mathbf{g}(\theta, \mathbf{z}, \mathbf{s})\langle \mathbf{t}(\mathbf{s})|v_J, \mathbf{x}_J\rangle\mathrm{d}\mathbf{s}, \tag{28}$$

respectively. Hereafter, to shortening the representations, the subscript $J = 0$, i ($i = 1, 2,...$) indicates the location of the point $\mathbf{x}_J$ inside either the matrix v_0 ($J = 0$) or the inclusion v_i ($J=i$; $i = 1, 2,...$); in so doing, $\mathbf{T}_0(\mathbf{x}-\mathbf{x}_0, \boldsymbol{\beta}_1)$ is taken as zero.

It is interesting to note that the conditional average stresses inside each component in the absence of a crack ($i = 1, 2,...$)

$$\langle \boldsymbol{\sigma}^{\mathrm{ac}}\rangle_i = \boldsymbol{\sigma}^0 + \mathbf{Q}_i\Big(\langle\boldsymbol{\beta}_1\rangle - \langle\boldsymbol{\beta}_1^{(i)}\rangle_i\Big) \tag{29}$$

$$\langle \boldsymbol{\sigma}^{\mathrm{ac}}\rangle_0 = \boldsymbol{\sigma}^0 + \frac{1}{c^{(0)}}\sum_{i=1}^{N} c^{(i)}\Big[\langle\mathbf{Q}_i\boldsymbol{\beta}_1^{(i)}\rangle_i - \mathbf{Q}_i\langle\boldsymbol{\beta}_1\rangle\Big], \tag{30}$$

do not depend on either of the conditional probability densities, $\varphi(v_p, \mathbf{x}_p|;v_i, \mathbf{x}_i)$ or $\varphi(v_p, \mathbf{x}_p|;v_0, \mathbf{x}_0)$, of the inclusion arrangement. At the same time, according to Eqs. (25) and (26), the conditional average of SIFs (Eqs. (27) and (28)) are explicitly expressed in terms of $\varphi(v_p, \mathbf{x}_p|;v_1, \mathbf{x}_i)$ and $\varphi(v_p, \mathbf{x}_p|;v_0, \mathbf{x}_0)$. For $\mathbf{x}_i$, $\mathbf{x}_0$ at infinity far from the point at the crack tip, Eqs. (27) and (28) lead to the vanishing results, $\langle \mathbf{K}^1(\mathbf{z})|v_i, \mathbf{x}_i\rangle = \langle \mathbf{K}^1(\mathbf{z})|v_0, \mathbf{x}_0\rangle = \langle \mathbf{K}^1(\mathbf{z})\rangle \equiv \mathbf{0}$, and the mean stresses inside each component are defined by Eqs. (29) and (30).

4. Conditional dispersion of SIF for a crack in the composite

To obtain the conditional second moment of the SIF and, consequently, the stresses in the neighborhood $\mathbf{x}\in v_i$ of the crack tip, it is necessary to take the tensor product of Eq. (18) into $\boldsymbol{\sigma}(\mathbf{x}|S, v_i, \mathbf{x}_i)$,

$$\boldsymbol{\sigma}(\mathbf{x}|S,\, v_i,\, \mathbf{x}_i) \otimes \boldsymbol{\sigma}(\mathbf{x}|S,\, v_i,\, \mathbf{x}_i) = \left[\boldsymbol{\sigma}^{\rm ac}(\mathbf{x}|v_i,\, \mathbf{x}_i) + \mathbf{J}(\theta,\, \mathbf{z}|v_i,\, \mathbf{x}_i)/\sqrt{\rho}\right] \otimes \left[\boldsymbol{\sigma}^{\rm ac}(\mathbf{x}|v_i,\, \mathbf{x}_i) + \mathbf{J}(\theta,\, \mathbf{z}|v_i,\, \mathbf{z}_i)/\sqrt{\rho}\right]. \tag{31}$$

Averaging Eq. (31) over the ensemble realization in terms of Eqs. (24) and (26) leads to the conditional expectation of Eq. (31), composed from three terms

$$\langle \boldsymbol{\sigma}(\mathbf{x}|S,\, v_i,\, \mathbf{x}_i) \otimes \boldsymbol{\sigma}(\mathbf{x}|S,\, v_i,\, \mathbf{x}_i)\rangle = \mathbf{I}_{20} + \mathbf{I}_{21} + \mathbf{I}_{22}. \tag{32}$$

The first term, $\mathbf{I}_{20}$, is determined by the second moment of stresses in the point $\mathbf{x} \in v_i$ in the absence of a crack (Eq. 4.3 in Buryachenko, 1999b)

$$\mathbf{I}_{20} \equiv \langle \boldsymbol{\sigma}^{\rm ac} \otimes \boldsymbol{\sigma}^{\rm ac}\rangle_i(\mathbf{x}) = \langle \boldsymbol{\sigma}^{\rm ac}\rangle_i \otimes \langle \boldsymbol{\sigma}^{\rm ac}\rangle_i + \int \left[\mathbf{T}_p(\mathbf{x} - \mathbf{x}_p,\, \boldsymbol{\beta}_1)\bar{v}_p\right] \otimes \left[\mathbf{T}_p(\mathbf{x} - \mathbf{x}_p,\, \boldsymbol{\beta}_1)\bar{v}_p\right] \times \phi(v_p,\, \mathbf{x}_p|;v_i,\, \mathbf{x}_i)\mathrm{d}\mathbf{x} + \int\int \left[\mathbf{T}_p(\mathbf{x} - \mathbf{x}_p,\, \boldsymbol{\beta}_1)\bar{v}_p\right] \otimes \left[\mathbf{T}_q(\mathbf{x} - \mathbf{x}_q,\, \boldsymbol{\beta}_1)\bar{v}_q\right]\varphi(v_p,\, \mathbf{x}_p|;v_i,\, \mathbf{x}_i) \times [\varphi(v_q,\, \mathbf{x}_q|;v_p,\, \mathbf{x}_p;v_i,\, \mathbf{x}_i) - \varphi(v_q,\, \mathbf{x}_q|;v_i,\, \mathbf{x}_i)]\mathrm{d}\mathbf{x}_q\, \mathrm{d}\mathbf{x}_p. \tag{33}$$

The second term, $\mathbf{I}_{21}$ Eq. (31), as opposed to $\mathbf{I}_{20}$, has a singularity, $\rho^{-1/2}$,

$$\mathbf{I}_{21}\sqrt{\rho} \equiv \langle \boldsymbol{\sigma}^{\rm ac}\rangle_i(\mathbf{x}) \otimes \langle \mathbf{J}(\theta,\, \mathbf{z})|v_i,\, x_i\rangle + \langle \mathbf{J}(\theta,\, \mathbf{z})|v_i,\, \mathbf{x}_i\rangle \otimes \langle \boldsymbol{\sigma}^{\rm ac}\rangle(\mathbf{x})_i + \int \Big\{ \left[\mathbf{T}_p(\mathbf{x} - \mathbf{x}_p,\, \boldsymbol{\beta}_1)\bar{v}_p\right] \otimes \mathbf{J}^1(\theta,\, \mathbf{z},\, v_p,\, \mathbf{x}_p) + \mathbf{J}^1(\theta,\, \mathbf{z},\, v_p,\, \mathbf{x}_p) \otimes \left[\mathbf{T}_p(\mathbf{x} - \mathbf{x}_p,\, \boldsymbol{\beta}_1)\bar{v}_p\right] \Big\} \varphi(v_p,\, \mathbf{x}_p|;v_i,\, \mathbf{x}_i)\mathrm{d}\mathbf{x}_p + \int \Big\{ \left[\mathbf{T}_p(\mathbf{x} - \mathbf{x}_p,\, \boldsymbol{\beta}_1)\bar{v}_p\right] \otimes \mathbf{J}^1(\theta,\, \mathbf{z},\, v_q,\, \mathbf{x}_q) + \mathbf{J}^1(\theta,\, \mathbf{z},\, v_p,\, \mathbf{x}_p) \otimes \left[\mathbf{T}_q(\mathbf{x} - \mathbf{x}_q,\, \boldsymbol{\beta}_1)\bar{v}_q\right] \Big\} \varphi(v_p,\, \mathbf{x}_p|;v_i,\, \mathbf{x}_i) \times [\varphi(v_q,\, \mathbf{x}_q|;v_p,\, \mathbf{x}_p;v_i,\, \mathbf{x}_i) - \varphi(v_q,\, \mathbf{x}_q|;v_i,\, \mathbf{x}_i)]\mathrm{d}\mathbf{x}_q\, \mathrm{d}\mathbf{x}_p. \tag{34}$$

Finally the third term, $\mathbf{I}_{22}$ Eq. (32), has a singularity, ρ^{-1},

$$\mathbf{I}_{22}\rho \equiv \langle \mathbf{J}(\theta,\, \mathbf{z})|v_i,\, \mathbf{x}_i\rangle \otimes \langle \mathbf{J}(\theta,\, \mathbf{z})|v_i,\, \mathbf{x}_i\rangle + \int \mathbf{J}^1(\theta,\, \mathbf{z},\, v_p,\, \mathbf{x}_p) \otimes \mathbf{J}^1(\theta,\, \mathbf{z},\, v_p,\, \mathbf{x}_p)\varphi(v_p,\, \mathbf{x}_p|;v_i,\, \mathbf{x}_i)\mathrm{d}\mathbf{x}_p + \int\int \mathbf{J}^1(\theta,\, \mathbf{z},\, v_p,\, \mathbf{x}_p) \otimes \mathbf{J}^1(\theta,\, \mathbf{z},\, v_q,\, \mathbf{x}_q)\varphi(v_p,\, \mathbf{x}_p|;v_i,\, \mathbf{x}_i)[\varphi(v_q,\, \mathbf{x}_q|;v_p,\, \mathbf{x}_p;v_i,\, \mathbf{x}_i) - \varphi(v_q,\, \mathbf{x}_q|;v_i,\, \mathbf{x}_i)]\mathrm{d}\mathbf{x}_q d\mathbf{x}_p. \tag{35}$$

The third term, $\mathbf{I}_{22}$ Eq. (32), is most important for the application to fracture mechanics because Eq. (32) is a conditional elastic energy, and the contribution of $\mathbf{I}_{20}$ and $\mathbf{I}_{21}$ to Rice's integral (Rice, 1985) equals zero. It is interesting to compare the relation $\mathbf{I}_{20}$ Eq. (33) and $\mathbf{I}_{22}$ Eq. (35). The first terms in the right hand sides of Eqs. (33) and (35) are defined by the conditional averages of stresses in the absence of a crack Eqs. (29) and (30), and by the conditional average of the principal part of the stresses in the neighborhood of the crack tip Eq. (21). The second and third terms on the right hand sides of Eqs. (33) and (35) are less trivial; they are the conditional covariance matrix of corresponding values.

If the matrix is located in the vicinity of a crack tip, then the covariance matrix of the principal part of the stresses Eq. (13) can be derived in much the same way as Eq. (35)

$$\langle \boldsymbol{\sigma}(\mathbf{x}|S,\, v_0,\, \mathbf{x}_0) \otimes \boldsymbol{\sigma}(\mathbf{x}|S,\, v_0,\, \mathbf{x}_0)\rangle \rho = \langle \mathbf{J}(\theta,\, \mathbf{z})|v_0,\, \mathbf{x}_0\rangle \otimes \langle \mathbf{J}(\theta,\, \mathbf{z})|v_0,\, \mathbf{x}_0\rangle + \int \mathbf{J}^1(\theta,\, \mathbf{z},\, v_p,\, \mathbf{x}_p)$$
$$\otimes \mathbf{J}^1(\theta,\, \mathbf{z},\, v_q,\, \mathbf{x}_q)\phi(v_p,\, \mathbf{x}_p|;v_0,\, \mathbf{x}_0)\mathrm{d}\mathbf{x}_p + \int\int \mathbf{J}^1(\theta,\, \mathbf{z},\, v_p,\, \mathbf{x}_p) \otimes \mathbf{J}^1(\theta,\, \mathbf{z},\, v_q,\, x_q) \tag{36}$$
$$\times\, \varphi(v_p,\, x_p,\, |;v_0,\, \mathbf{x}_0)[\varphi(v_q,\, \mathbf{x}_q,\, |;v_p,\, \mathbf{x}_p;v_0,\, \mathbf{x}_0) - \varphi(v_q,\, \mathbf{x}_q|;v_0,\, \mathbf{x}_0)]\, \mathrm{d}\mathbf{x}_q\, \mathrm{d}\mathbf{x}_p,$$

where $\langle \mathbf{J}(\theta,\, \mathbf{z})|v_0,\, \mathbf{x}_0\rangle$ can be found in a manner like Eqs. (26) and (29).

After the production of Eqs. (35) and (36), it is an easy matter to obtain the conditional second moment of SIF $\langle \mathbf{K}(\mathbf{z}|v_i,\, \mathbf{x}_i) \otimes \mathbf{K}(\mathbf{z}|v_i,\, \mathbf{x}_i)\rangle$, $\langle \mathbf{K}(\mathbf{z}|v_0,\, \mathbf{x}_0) \otimes \mathbf{K}(\mathbf{z}|v_0,\, \mathbf{x}_0)\rangle$ for $\mathbf{x}_1$ and $\mathbf{x}_0$ are infinitely far from the crack tip. Evidently, SIF does not depend on the coordinate of the fixed point $\langle \mathbf{K}(\mathbf{z}|v_i,\, \mathbf{x}_i) \otimes \mathbf{K}(\mathbf{z}|v_i,\, \mathbf{x}_i)\rangle \to \langle \mathbf{K}(\mathbf{z}) \otimes \mathbf{K}(\mathbf{z})\rangle = \text{const.} \neq \mathbf{K}^0(\mathbf{z}) \otimes \mathbf{K}^0(\mathbf{z})$ and $\langle \mathbf{K}(\mathbf{z}|v_0,\ \mathbf{x}_0) \otimes \mathbf{K}(\mathbf{z}|v_0,\ \mathbf{x}_0)\rangle \to \langle \mathbf{K}(\mathbf{z}) \otimes \mathbf{K}(\mathbf{z})\rangle = \text{const.} \neq \mathbf{K}^0(\mathbf{z}) \otimes \mathbf{K}^0(\mathbf{z})$, respectively.

5. Statistical moments of arbitrary orders for the tensor SIF

The estimation method of the second moments of the tensor SIF (Eqs. (33) and (36)) is used to evaluate the statistical moments of any order of the tensor SIF. For example, for the third order moment, we take the tensor product of Eq. (31) into $\boldsymbol{\sigma}(\mathbf{x}|S,\, v_i,\, \mathbf{x}_i)$, $\mathbf{x} \in v_i$,

$$\boldsymbol{\sigma}(\mathbf{x}|S,\, v_i,\, \mathbf{x}_i) \otimes \boldsymbol{\sigma}(\mathbf{x}|S,\, v_i,\, \mathbf{x}_i) \otimes \boldsymbol{\sigma}(\mathbf{x}|S,\, v_i,\, \mathbf{x}_i) = \left[\boldsymbol{\sigma}^{\mathrm{ac}}(\mathbf{x}|v_i,\, \mathbf{x}_i) + \mathbf{J}(\theta,\, \mathbf{z}|v_i,\, \mathbf{x}_i)/\sqrt{\rho}\right]$$
$$\otimes \left[\boldsymbol{\sigma}^{\mathrm{ac}}(\mathbf{x}|v_i,\, \mathbf{x}_i) + \mathbf{J}(\theta,\, \mathbf{z}|v_i,\, \mathbf{x}_i)/\sqrt{\rho}\right] \otimes \left[\boldsymbol{\sigma}^{\mathrm{ac}}(\mathbf{x}|v_i,\, \mathbf{x}_i) + \mathbf{J}(\theta,\, \mathbf{z}|v_i,\, \mathbf{x}_i)/\sqrt{\rho}\right]. \tag{37}$$

For simplicity's sake, only the binary interaction of the inclusions are taken into account for the integral equation Eq. (37). When one averages Eq. (37) over realization of the ensemble inclusions with regard to Eq. (32), we obtain

$$\langle \boldsymbol{\sigma}(\mathbf{x}|S,\, v_i,\, \mathbf{x}_i) \otimes \boldsymbol{\sigma}(\mathbf{x}|S,\, v_i,\, \mathbf{x}_i) \otimes \boldsymbol{\sigma}(\mathbf{x}|S,\, v_i,\, \mathbf{x}_i)\rangle = \mathbf{I}_{30} + \mathbf{I}_{31} + \mathbf{I}_{32} + \mathbf{I}_{33}, \tag{38}$$

where the terms $\mathbf{I}_{3q}$ ($q = 0, 1, 2, 3$) have the singularities, $\rho^{-q/2}$.

The therm of greatest practical utility is a principal part of stresses $\mathbf{I}_{33}$ which can be represented in the index form (Voigt's notation $k, l, m = 1,..., 6$)

$$I_{33klm} = \rho^{-3/2}\big\{\langle J_k(\theta,\, \mathbf{z})|v_i,\, \mathbf{x}_i\rangle \otimes \langle J_l(\theta,\, \mathbf{z})|v_i,\, \mathbf{x}_i\rangle \otimes \langle J_m(\theta,\, \mathbf{z})|v_i,\, \mathbf{x}_i\rangle + \Delta J^2_{kl}(\theta,\, \mathbf{z}|v_i,\, \mathbf{x}_i)$$
$$\otimes \langle J_m(\theta,\, \mathbf{z})|v_i,\, \mathbf{x}_i\rangle + \Delta J^2_{km}(\theta,\, \mathbf{z}|v_i,\, \mathbf{x}_i) \otimes \langle J_l(\theta,\, \mathbf{z})|v_i,\, \mathbf{x}_i\rangle + \Delta J^2_{lm}(\theta,\, \mathbf{z}|v_i,\, \mathbf{x}_i) \tag{39}$$
$$\otimes \langle J_k(\theta,\, \mathbf{z})|v_i,\, \mathbf{x}_i\rangle + \Delta J^3_{klm}(\theta,\, \mathbf{z}|v_i,\, \mathbf{x}_i)\big\},$$

where, taking Eq. (32) into account, the tensor $\Delta\mathbf{J}^2(\theta,\, \mathbf{z}|v_i,\, \mathbf{x}_i)$ is defined by both the double and triple correlation functions of the inclusions,

$$\Delta\mathbf{J}^2(\theta,\, \mathbf{z}|v_i,\, \mathbf{x}_i) = \int \mathbf{J}^1(\theta,\, \mathbf{z},\, v_p,\, \mathbf{x}_p) \otimes \mathbf{J}^1(\theta,\, \mathbf{z},\, v_q,\, \mathbf{x}_q) \cdot \phi(v_p,\, \mathbf{x}_p|;v_0,\, \mathbf{x}_0)\mathrm{d}\mathbf{x}_p + \int\int \mathbf{J}^1(\theta,\, \mathbf{z},\, v_p,\, \mathbf{x}_p)$$
$$\otimes \mathbf{J}^1(\theta,\, \mathbf{z},\, v_q,\, x_q)\varphi(v_p,\, x_p,\, |;v_0,\, \mathbf{x}_0) \cdot [\varphi(v_q,\, \mathbf{x}_q,\, |;v_p,\, \mathbf{x}_p;\, v_0,\, \mathbf{x}_0) - \varphi(v_q,\, \mathbf{x}_q|;v_0,\, \mathbf{x}_0)]\mathrm{d}\mathbf{x}_q\, \mathrm{d}\mathbf{x}_p. \tag{40}$$

The following approximation for the tensor $\Delta\mathbf{J}^3(\theta,\, \mathbf{z}|v_i,\, \mathbf{x}_i)$ can be obtained by taking into account

only the binary interaction of inclusions

$$\Delta\mathbf{J}^3(\theta, \mathbf{z}|v_i, \mathbf{x}_i) \equiv \int \mathbf{J}^1(\theta, \mathbf{z}, v_p, \mathbf{x}_p) \otimes \mathbf{J}^1(\theta, \mathbf{z}, v_p, \mathbf{x}_p) \otimes \mathbf{J}^1(\theta, \mathbf{z}, v_p, \mathbf{x}_p) \otimes \varphi(v_p, \mathbf{x}_p|; v_i, \mathbf{x}_i)\mathrm{d}\mathbf{x}_p. \tag{41}$$

The omitted terms in Eq. (41) have the second order of smallness over c.

It is interesting to compare a Gaussian distribution and distribution law of real stresses inside the inclusions. Let the notation $\Delta^{\mathrm{G}}\langle\mathbf{e}\otimes\ldots\otimes\mathbf{e}\rangle \equiv \langle\mathbf{e}\otimes\ldots\otimes\mathbf{e}\rangle - \langle\mathbf{e}^{\mathrm{G}}\otimes\ldots\otimes\mathbf{e}^{\mathrm{G}}\rangle$ denotes the difference of the moments of the real random variable $\langle\mathbf{e}\otimes\ldots\otimes\mathbf{e}\rangle$ and its Gaussian approximation $\langle\mathbf{e}^{\mathrm{G}}\otimes\ldots\otimes\mathbf{e}^{\mathrm{G}}\rangle$, having a Gaussian probability density with the first and second statistical moments of the random variable $\mathbf{e}$. We will consider a dissimilar $\Delta^{\mathrm{G}}\langle\mathbf{J}(\theta, \mathbf{z}|v_i, \mathbf{x}_i) \otimes \mathbf{J}(\theta, \mathbf{z}|v_i, \mathbf{x}_i) \otimes \mathbf{J}(\theta, \mathbf{z}|v_i, \mathbf{x}_i)\rangle$ between the Gaussian distribution $\langle\mathbf{J}^{\mathrm{G}}(\theta, \mathbf{z}|v_i, \mathbf{x}_i) \otimes \mathbf{J}^{\mathrm{G}}(\theta, \mathbf{z}|v_i, \mathbf{x}_i) \otimes \mathbf{J}^{\mathrm{G}}(\theta, \mathbf{z}|v_i, \mathbf{x}_i)\rangle$ and the distribution of the real tensor SIF in the same manner as statistical stress moments inside the components have been analyzed in the preceding paper (see Eq. 5.9 in Buryachenko, 1999b). The comparison of Eq. (39) with the third statistical moment of the Gaussian distribution gives

$$\Delta^{\mathrm{G}}\langle\mathbf{J}(\theta, \mathbf{z}|v_i, \mathbf{x}_i) \otimes \mathbf{J}(\theta, \mathbf{z}|v_i, \mathbf{x}_i) \otimes \mathbf{J}(\theta, \mathbf{z}|v_i, \mathbf{x}_i)\rangle = \Delta\mathbf{J}^3(\theta, \mathbf{z}|v_i, \mathbf{x}_i). \tag{42}$$

Similar reasoning shows that in the framework of binary interactions of inclusions, the principal part of a correction of n-th order to the Gaussian approximation, $\langle\mathbf{J}^{\mathrm{G}}(\theta, \mathbf{z}|v_i, \mathbf{x}_i)[\otimes\mathbf{J}^{\mathrm{G}}(\theta, \mathbf{z}|v_i, \mathbf{x}_i)]^{n-1}\rangle$, can be represented as

$$\begin{aligned}\Delta^{\mathrm{G}}\langle\mathbf{J}(\theta, \mathbf{z}|v_i, \mathbf{x}_i)[\otimes\mathbf{J}(\theta, \mathbf{z}|v_i, \mathbf{x}_i)]^{n-1}\rangle = \Delta\mathbf{J}^n(\theta, \mathbf{z}|v_i, \mathbf{x}_i) \equiv \int \mathbf{J}^1(\theta, \mathbf{z}, v_p, \mathbf{x}_p) \\ \times [\otimes\mathbf{J}^1(\theta, \mathbf{z}, v_p, \mathbf{x}_p)]^{n-1}\varphi(v_p, \mathbf{x}_p|; v_i, \mathbf{x}_i)\mathrm{d}\mathbf{x}_p.\end{aligned} \tag{43}$$

If in Eqs. (39), (40), (41), (42) and (43), the index i is changed to 0, we will obtain the pertinent results for the statistical moments of the tensor SIF under the condition $\mathbf{x}, \mathbf{x}_0 \in v_0$.

6. Crack in a finite inclusion cloud

Within a wealth of practical problems, there is a need for an analysis of the finite inclusion field. So the high stresses in the vicinity of macroscopic crack induce a transformation toughening of zirconia (ZrO_2) inclusions embedded in a matrix of non-transforming ceramic. When ZrO_2 particles are unconstrained by the surrounding matrix, their transformation from tetragonal to a monoclinic crystal structure can be decomposed into a volume expansion of 4% and a shear of about 16% (Budiansky et al., 1983; Lambropoulos, 1986). This transformation, in turn, alters the stress distribution near the crack tip. In this connection, we will consider the case of a statistically inhomogeneous inclusion field, when number probability density is a function of current coordinate and equals zero outside of some domain w^{fin} with characteristic function W^{fin}.

Then, in much the same manner as Buryachenko and Parton (1990a, 1990b), and Wang (1990), one can obtain a general equation for random stresses at any point in the absence of a crack (denoted by the superscript 'ac')

$$\boldsymbol{\sigma}^{\mathrm{ac}}(\mathbf{x}) = \boldsymbol{\sigma}^0 + \int \boldsymbol{\Gamma}(\mathbf{x}-\mathbf{y})\boldsymbol{\beta}_1(\mathbf{y})\mathrm{d}\mathbf{y} \tag{44}$$

$$\boldsymbol{\sigma}^{\rm ac}(\mathbf{x}) = \langle\boldsymbol{\sigma}^{\rm ac}\rangle(\mathbf{x}) + \int \boldsymbol{\Gamma}(\mathbf{x}-\mathbf{y})[\boldsymbol{\beta}_1(\mathbf{y}) - \langle\boldsymbol{\beta}_1\rangle(\mathbf{y})]d\mathbf{y}. \tag{45}$$

Here, the average stress $\langle\boldsymbol{\sigma}^{\rm ac}\rangle(\mathbf{x}) \not\equiv \boldsymbol{\sigma}^0$, in contrast to the statistically homogeneous structure, and can be defined by the relation

$$\langle\boldsymbol{\sigma}^{\rm ac}\rangle(\mathbf{x}) = \boldsymbol{\sigma}^0 + \int \boldsymbol{\Gamma}(\mathbf{x}-\mathbf{y})\langle\boldsymbol{\beta}_1\rangle(\mathbf{y})d\mathbf{y}. \tag{46}$$

Hereafter, the notation $\langle(\cdot)\rangle(\mathbf{x})$ denotes the statistical average in the point $\mathbf{x}$ over the ensemble realization of the statistically inhomogeneous inclusion field. If $\langle\boldsymbol{\beta}_1\rangle(\mathbf{y}) \equiv \langle\boldsymbol{\beta}_1\rangle = \text{const.}$ in some finite domain $w^{\rm fin}$, Eq. (46) may be simplified to

$$\langle\boldsymbol{\sigma}^{\rm ac}\rangle(\mathbf{x}) = \boldsymbol{\sigma}^0 + \int \boldsymbol{\Gamma}(\mathbf{x}-\mathbf{y})W^{\rm fin}(\mathbf{y})d\mathbf{y}\langle\boldsymbol{\beta}_1\rangle. \tag{47}$$

If besides, $w^{\rm fin}$ is an ellipsoid with the center $\mathbf{x}^{\rm fin}$, then

$$\langle\boldsymbol{\sigma}^{\rm ac}\rangle(\mathbf{x}) = \begin{cases} \boldsymbol{\sigma}^0 - \mathbf{Q}(w^{\rm fin})\langle\boldsymbol{\beta}_1\rangle, & \mathbf{x} \in w^{\rm fin} \\ \boldsymbol{\sigma}^0 + \mathbf{T}^{\rm fin}(\mathbf{x}-\mathbf{x}^{\rm fin})\langle\boldsymbol{\beta}_1\rangle\bar{w}^{\rm fin}, & \mathbf{x}\notin w^{\rm fin} \end{cases}, \tag{48}$$

where $\mathbf{T}^{\rm fin}(\mathbf{x}-\mathbf{x}^{\rm fin})$ and $\mathbf{Q}(w^{\rm fin})$ are defined by Eqs. (7) and (8) with replacement of v_i by $w^{\rm fin}$.

From comparison of Eqs. (19) and (45), we see that the analysis of the finite inclusion cloud $w^{\rm fin}$ is formally reduced to the replacement of $\boldsymbol{\sigma}^0$ on the determinate terms $\langle\boldsymbol{\sigma}^{\rm ac}\rangle(\mathbf{x})$ in Eq. (45). Of course, as this takes place, the number probability density, $\phi(v_i, \mathbf{x}_i)$, and the conditional density, $\phi(v_p, \mathbf{x}_p|;v_i, \mathbf{x}_i)$, determining the values of the right-hand-side integrals in Eqs. (45) and (46), are functions of a coordinate $\mathbf{x}_i$ and are not invariants with respect to translations $\mathbf{x}_i \longrightarrow \mathbf{x}_i + \mathbf{y}$.

Thus we obtain the estimations for both the average SIFs and the average tensor SIFs

$$\langle\mathbf{K}(\mathbf{z})\rangle = \mathbf{K}(\langle\boldsymbol{\sigma}^{\rm ac}\rangle, \mathbf{z}) \equiv -\int_S \mathbf{k}(\mathbf{z}, \mathbf{s})\mathbf{n}(\mathbf{s})\langle\boldsymbol{\sigma}^{\rm ac}\rangle(\mathbf{s})d\mathbf{s}, \tag{49}$$

$$\langle\mathbf{J}(\theta, \mathbf{z})\rangle = \mathbf{J}(\langle\boldsymbol{\sigma}^{\rm ac}\rangle, \theta, \mathbf{z}) \equiv -\int_S \mathbf{g}(\theta, \mathbf{z},\mathbf{s})\mathbf{n}(\mathbf{s})\langle\boldsymbol{\sigma}^{\rm ac}\rangle(\mathbf{s})d\mathbf{s}. \tag{50}$$

For example, for the crack tip inside the statistically homogeneous inclusion cloud $w^{\rm fin}$, having an ellipsoidal shape, we have

$$\langle\mathbf{K}(\mathbf{z})\rangle = \mathbf{K}^0(\mathbf{z}) - \int_S \mathbf{k}(\mathbf{z}, \mathbf{s})\mathbf{n}(\mathbf{s})W(\mathbf{s})d\mathbf{s}\mathbf{Q}(w^{\rm fin})\langle\boldsymbol{\beta}_1\rangle. \tag{51}$$

This reproduces the known results from the two-dimensional models developed in the literature on transformation toughening of ceramics (McMeeking and Evans, 1982; Lambropoulos, 1986; Stump and Budiansky, 1989). Eq. (51) does not depend on the microgeometric structure of he composite and is correct for the case when the distance between the crack tip and the cloud boundary is large enough.

However, the local distribution of the stresses near the crack tip plays a crucial role in linear fracture mechanics. Because of this let us now turn to the estimations of conditional expectation values of both the SIF and the tensor SIF. With this aim in view, the conditional expectation of stress values can be found in much the same way as Eqs. (22) and (24)

$$\langle\boldsymbol{\sigma}^{\rm ac}(\mathbf{x})|v_J,\mathbf{x}_J\rangle=\langle\boldsymbol{\sigma}^{\rm ac}\rangle(\mathbf{x})+\mathbf{T}_J(\mathbf{x}-\mathbf{x}_J,\boldsymbol{\beta}_1)\bar{v}_J+\int\big[\mathbf{T}_p(\mathbf{x}-\mathbf{x}_p,\boldsymbol{\beta}_1)\bar{v}_p\varphi(v_p,\mathbf{x}_p|;v_J,\mathbf{x}_J)-\boldsymbol{\Gamma}(\mathbf{x}-\mathbf{x}_p)\langle\boldsymbol{\beta}_1\rangle(\mathbf{x}_p)\big]{\rm d}\mathbf{x}_p, \tag{52}$$

where the subscript $J=0$, i ($i=1,2,...$) indicates the location of the point $\mathbf{x}_J$ inside either the matrix, v_0 ($J=0$), or the inclusion, v_i ($J=i$; $i=1,2,...$). Contrary to Eqs. (22) and (24), the right-hand-side of Eq. (52) consists of both the average stresses, $\langle\boldsymbol{\sigma}^{\rm ac}\rangle\not\equiv\boldsymbol{\sigma}^0$ estimated above by Eq. (46) and the macroscopically inhomogeneous deterministic tensor, $\langle\boldsymbol{\beta}_1\rangle(\mathbf{x}_p)$, describing the statistical inhomogeneous transformed field. Substituting Eq. (52) into Eq. (4) gives the conditional expectation of the value of the tensor SIF

$$\langle\mathbf{J}(\theta,\mathbf{z})|v_J,\mathbf{x}_J\rangle=\langle\mathbf{J}^{\rm fluct}(\theta,\mathbf{z})|v_J,\mathbf{x}_J\rangle+\langle\mathbf{J}(\langle\boldsymbol{\sigma}^{\rm ac}\rangle,\theta,\mathbf{z})\rangle,\ (J=0,\ i;i=1,2,\ldots), \tag{53}$$

where the average tensor SIF $\langle\mathbf{J}(\langle\boldsymbol{\sigma}^{\rm ac}\rangle,\ \theta,\ \mathbf{z})\rangle\not\equiv\mathbf{J}^0(\theta,\ \mathbf{z})$ is estimated by Eqs. (46) and (50) for the macroscopically inhomogeneous cloud $w^{\rm fin}$ with the deterministic transformed field $\langle\boldsymbol{\beta}_1\rangle(\mathbf{x})$. The fluctuating constituent term $\langle\mathbf{J}^{\rm fluct}(\theta,\mathbf{z})|v_J,\mathbf{x}_J\rangle$ ($J=0$, i; $i=1,2...$) is defined by the formula

$$\langle\mathbf{J}^{\rm fluct}(\theta,\mathbf{z})|v_J,\mathbf{x}_J\rangle=-\int_S\mathbf{g}(\theta,\mathbf{z},\mathbf{s})\mathbf{n}(\mathbf{s})\Big\{\mathbf{T}_J(\mathbf{x}-\mathbf{x}_J,\boldsymbol{\beta}_1)\bar{v}_J+\int\big[\mathbf{T}_p(\mathbf{x}-\mathbf{x}_p,\boldsymbol{\beta}_1)\cdot\bar{v}_p\varphi(v_p,\mathbf{x}_p|;v_J,\mathbf{x}_J)-\boldsymbol{\Gamma}(\mathbf{x}-\mathbf{x}_p)\langle\boldsymbol{\beta}_1\rangle(\mathbf{x}_p)\big]{\rm d}\mathbf{x}_p\Big\}{\rm d}\mathbf{s} \tag{54}$$

and formally coincides with a similar representation for a statistically homogeneous infinite inclusion field, although at the considered juncture, the probability densities $\phi(v_i,\mathbf{x}_i)$ and $\phi(v_p,\mathbf{x}_p|;v_J,\mathbf{x}_J)$ ($J=0$, i; $i=1,2,...$) are insensitive to translations.

Repeating the derivation of Eqs. (35) and (36) gives the covariance matrix of the principal part of the conditional average stresses in the components ($J=0$, i)

$$\langle\boldsymbol{\sigma}(\mathbf{x}|S,v_J,\mathbf{x}_J)\otimes\boldsymbol{\sigma}(\mathbf{x}|S,v_J,\mathbf{x}_J)\rangle=\frac{1}{\rho}\langle\mathbf{J}(\theta,\mathbf{z})|v_J,\mathbf{x}_J\rangle\otimes\langle\mathbf{J}(\theta,\mathbf{z})|v_J,\mathbf{x}_J\rangle+\frac{1}{\rho}\int\mathbf{J}^1(\theta,\mathbf{z},v_p,\mathbf{x}_p)\otimes\mathbf{J}^1(\theta,\mathbf{z},v_p,\mathbf{x}_p)\varphi(v_p,\mathbf{x}_p|;v_J,\mathbf{x}_J){\rm d}\mathbf{x}_p+\frac{1}{\rho}\int\int\mathbf{J}^1(\theta,\mathbf{z},v_p,\mathbf{x}_p)\otimes\mathbf{J}^1(\theta,\mathbf{z},v_q,\mathbf{x}_q)\varphi(v_p,\mathbf{x}_p|;v_J,\mathbf{x}_J)\cdot[\varphi(v_q,\mathbf{x}_q|;v_p,\mathbf{x}_p;v_J,\mathbf{x}_J)-\varphi(v_q,\mathbf{x}_q|;v_J,\mathbf{x}_J)]{\rm d}\mathbf{x}_q\,{\rm d}\mathbf{x}_p, \tag{55}$$

where $\langle\mathbf{J}(\theta,\mathbf{z})|v_J,\mathbf{x}_J\rangle$ is defined by Eq. (53), and $\mathbf{J}^1(\theta,\mathbf{z},v_p,\mathbf{x}_p)$ describes the impact of a single isolated inclusion on the stress distribution in the vicinity of a crack tip Eq. (12). As can be shown in a concrete numerical example, the conditional average $\langle\boldsymbol{\sigma}|v_i,\mathbf{x}_i\rangle(\mathbf{x})$ for $\mathbf{x}\in v_i\subset w^{\rm fin}$ can differ significantly from the statistical average $\langle\boldsymbol{\sigma}\rangle(\mathbf{x})$, which leads to all the more difference between estimation obtained by use of the popular Eq. (50) as compared to the more accurate Eqs. (53) and (55).

7. Crack in regular inclusion field

At the present time, high-efficiency numerical methods are developed for calculation of effective properties and stress distribution inside composites of regular structures (see, as an example, the survey in Walker et al., 1990; Bensoussan et al., 1978). It turns out that for elastically homogeneous composites, the noted problem can be solved simply and exactly in the context of the theory at hand in

conjunction with Buryachenko and Parton (1992a, 1992b) (see also Buryachenko, 1999a). In fact, let us consider a spatial grid of ellipsoidal inclusions with the same form, orientation and stress-free strains which are located in the nodes of this grid. Suppose $\mathbf{e}_k$ ($k = 1, 2, 3$) are linearly-independent vectors of the principal period of the grid, so that any node $\mathbf{x}_i$ may be represented in the form

$$\mathbf{x}_i = \sum_{k=1}^{3} m_k^i \mathbf{e}_k, \ (i = 1, 2, \ldots), \tag{56}$$

where m_k^i are integer-valued coordinates of the node $\mathbf{x}_i$ in the periodic basis ($\mathbf{e}_k$). Then the general equation for the stresses Eq. (45) in any point $\mathbf{x}$, in the absence of a crack, will take the form

$$\boldsymbol{\sigma}^{\mathrm{ac}}(\mathbf{x}) = \boldsymbol{\sigma}^0 - \mathbf{Q}_i(\mathbf{x}, \boldsymbol{\beta}_1) + \mathbf{Q}(w^{\mathrm{fin}})\langle\boldsymbol{\beta}_1\rangle + \sum_{i\neq j} \mathbf{T}_j(\mathbf{x} - \mathbf{x}_j, \boldsymbol{\beta}_1)\bar{v}_j \tag{57}$$

for $\mathbf{x} \in v_i$ and

$$\boldsymbol{\sigma}^{\mathrm{ac}}(\mathbf{x}_0) = \boldsymbol{\sigma}^0 + \mathbf{Q}(w^{\mathrm{fin}})\langle\boldsymbol{\beta}_1\rangle + \sum_{j} \mathbf{T}_j(\mathbf{x}_0 - \mathbf{x}_j, \boldsymbol{\beta}_1)\bar{v}_j \tag{58}$$

at $\mathbf{x} \in v_0$. In Eqs. (57) and (58), we take into account that $\mathbf{x}_i$ coincides with the center of some ellipsoidal domain w^{fin}, which contains a reasonably large number of inclusions; $\mathbf{x}$ lies inside the periodic cell $\Omega_i \ni v_i$. In Eqs. (57) and (58), the summation is over all $\mathbf{x}_j \in w^{\mathrm{fin}}$, in view of $\mathbf{x}_j \neq \mathbf{x}_i$ in Eq. (57); the form and the size (for a sufficiently large size of the domain w^{fin}) have no influence on the calculated stresses (Eqs. (57) and (58)).

After obtaining the periodic determined stress field, $\boldsymbol{\sigma}^{\mathrm{ac}}(\mathbf{x})$ (Eqs. (57) and (58)) and therefore $\mathbf{t}(\mathbf{s})$, SIF can be found by the use of Eq. (3). Of course in the determinate case being analyzed, $\Delta\mathbf{J}^2(\theta, \mathbf{z}|v_i, \mathbf{x}_i) \equiv 0$.

8. Effective limiting surfaces of composite materials

8.1. Effective strength surface

Let us assume that the tensor–polynomial strength criterion is defined for each component, i.e.

$$\boldsymbol{\Pi}(\boldsymbol{\sigma}) = \boldsymbol{\Pi}^{2(i)}\boldsymbol{\sigma} + \boldsymbol{\Pi}^{4(i)}(\boldsymbol{\sigma}\otimes\boldsymbol{\sigma}) + \boldsymbol{\Pi}^{6(i)}(\boldsymbol{\sigma}\otimes\boldsymbol{\sigma}\otimes\boldsymbol{\sigma}) + \ldots = 1, \tag{59}$$

where $i = 0,1,...$, and the second-, fourth- and sixth-rank tensors of strength $\boldsymbol{\Pi}^2$, $\boldsymbol{\Pi}^4$ and $\boldsymbol{\Pi}^6$ are expressed through technical strength parameters for different classes of material symmetry (Theocaris, 1991; Jang and Tennysin, 1989).

Note, that a common way to produce effective strength of a surface is substitution of the component average stress values into Eq. (59) ($i = 0, 1,...$) (Arsenault and Taya, 1987; Reifsnider and Gao, 1991)

$$\boldsymbol{\Pi}^*(\boldsymbol{\sigma}) = \max_i \left[\boldsymbol{\Pi}^{2(i)}\langle\boldsymbol{\sigma}\rangle_i + \boldsymbol{\Pi}^{4(i)}(\langle\boldsymbol{\sigma}\rangle_i\otimes\langle\boldsymbol{\sigma}\rangle_i) + \boldsymbol{\Pi}^{6(i)}(\langle\boldsymbol{\sigma}\rangle_i\otimes\langle\boldsymbol{\sigma}\rangle_i\otimes\langle\boldsymbol{\sigma}\rangle_i) + \ldots\right] = 1. \tag{60}$$

As this takes place, the strength criteria in Eq. (60) brings us to physically inconsistant results, which will be shown later.

It seems that the following definition of effective surface strength will be more correct

$$\mathbf{\Pi}^{*}(\boldsymbol{\sigma}) = \max_{i} \left[\mathbf{\Pi}^{2(i)} \langle \boldsymbol{\sigma} \rangle_i + \mathbf{\Pi}^{4(i)} \langle \boldsymbol{\sigma} \otimes \boldsymbol{\sigma} \rangle_i + \mathbf{\Pi}^{6(i)} \langle \boldsymbol{\sigma} \otimes \boldsymbol{\sigma} \otimes \boldsymbol{\sigma} \rangle_i + \dots \right] = 1, \tag{61}$$

where the estimations of average stress moments of different orders, $\langle \boldsymbol{\sigma} \rangle_i$, $\langle \boldsymbol{\sigma} \otimes \boldsymbol{\sigma} \rangle_i$, $\langle \boldsymbol{\sigma} \otimes \boldsymbol{\sigma} \otimes \boldsymbol{\sigma} \rangle_i$ ($i = 0$, 1,...), can be found by use of the relevant formulae from Buryachenko (1999b).

If the possibility of interfacial fracture is taken into account, the macrostrength criterion can be express in the following form ($i = 0$, 1,...)

$$\begin{aligned} \mathbf{\Pi}_a^{*}(\boldsymbol{\sigma}) = \max \Bigg\{ & \mathbf{\Pi} * (\langle \boldsymbol{\sigma} \rangle), \max_i \max_{\mathbf{n}} \Big[\mathbf{\Pi}_a^{2(i)} \langle \boldsymbol{\sigma}^{-}(\mathbf{n}) \rangle_x + \mathbf{\Pi}_a^{4(i)} \langle \boldsymbol{\sigma}^{-}(\mathbf{n}) \otimes \boldsymbol{\sigma}^{-}(\mathbf{n}) \rangle_x \\ & + \mathbf{\Pi}_a^{6(i)} \langle \boldsymbol{\sigma}^{-}(\mathbf{n}) \otimes \boldsymbol{\sigma}^{-}(\mathbf{n}) \otimes \boldsymbol{\sigma}^{-}(\mathbf{n}) \rangle_x + \dots \Big] \Bigg\} = 1, \end{aligned} \tag{62}$$

where $\langle \boldsymbol{\sigma}^{-}(\mathbf{n}) \rangle_x$, $\langle \boldsymbol{\sigma}^{-}(\mathbf{n}) \otimes \boldsymbol{\sigma}^{-}(\mathbf{n}) \rangle_x$ and $\langle \boldsymbol{\sigma}^{-}(\mathbf{n}) \otimes \boldsymbol{\sigma}^{-}(\mathbf{n}) \otimes \boldsymbol{\sigma}^{-}(\mathbf{n}) \rangle_x$ are the statistical moments of limiting stresses within the matrix near the inclusion boundary $\mathbf{x} \in \partial v_i$, with the unit outward normal vector $\mathbf{n}$ (Eq. 5.14 in Buryachenko, 1999b). Generally speaking, the adhesion strength parameters, $\mathbf{\Pi}_a^{2(i)}$, $\mathbf{\Pi}_a^{4(i)}$ and $\mathbf{\Pi}_a^{6(i)}$ differ from $\mathbf{\Pi}^{2(i)}$, $\mathbf{\Pi}^{4(i)}$ and $\mathbf{\Pi}^{6(i)}$.

Let us show the physical consistency of the effective strength criterion (Eqs. (61) and (4)) (in contrast to Eq. (60)). In fact, let us consider a two-component isotropic composite with isotropic ones. In this case, one may observe that symmetry requires that the average stresses inside both components will be hydrostatic; one $\langle \sigma_{kl} \rangle_1 \equiv \langle \sigma_{kl} \rangle_0 (1 - c)/c \equiv \sigma_{11}^0 \delta_{kl}$; in so doing, the microstructure of, and the method of calculation of, the average stresses inside the components (for example, Eq. 3.8 in Buryachenko, 1999b; or any other formula) influence the value of the scalar σ_{11}^0, but have no effect on the tensor structure of the fields, $\langle \boldsymbol{\sigma} \rangle_0$ and $\langle \boldsymbol{\sigma} \rangle_1$. Then the composite strength is dictated by the strength of the component which is to be found under conditions of hydrostatic tension and is not determined by the strength of the second component. If the strength of the second component falls far short of the strength of the first, we will obtain improper prediction of composite strength. In fact, according to Eqs. 4.5 and 4.15 in Buryachenko, 1999a, 1999b, the average values of the second deviator invariant inside each component $\langle \mathbf{ss} \rangle_i \neq 0$ ($s_{kl} \equiv \sigma_{kl} - \sigma_{mm} \delta_{kl}/3$; $i = 0$, 1,...). Therefore, the composite strength is defined by the strength of the second, weaker component at the cost of the fluctuations of the stress deviator.

8.2. Effective energy release rate of an isolated crack in the composite

Let us consider a penny-shaped crack of radius R^{c} with center $\mathbf{x}^{c} = (0, 0, 0)$ and unit normal $\mathbf{n} = (1, 0, 0)$ to the crack surface S in an infinite elastic homogeneous medium. The energy release rate may be defined by means of $\mathbf{K} \equiv (K_1, K_2, K_3)^{\top}$

$$\mathscr{J} = \mathbf{\Lambda}(\mathbf{K} \otimes K), \tag{63}$$

where, for the general anisotropic, material the matrix Λ_{ij} ($i, j = 1, 2, 3$) is symmetric (see Barnett and Asaro, 1972; Rice, 1989). For an isotropic material, the matrix Λ_{ij} Eq. (63) is diagonal

$$\mathbf{\Lambda} = (2\mu)^{-1} \operatorname{diag}(1 - \nu, 1 - \nu, 1). \tag{64}$$

The energy release rate, $\mathscr{J}$, could alternatively expressed as a path-independent line J^{r} Rice's integral, which is invariant with respect to the integration along an arbitrary path encircling the crack tip (see, e.g. Nied, 1994; Wilson and Yu, 1979).

The energy rate $\mathscr{J}$ provides a means to introduce a crack propagation criterion on a physical basis: a crack can propagate if the potential energy released per unit area of newly created crack surface exceeds

the work which is consumed in creating this new amount of surface. The fracture criterion that will be used for the remainder of this work is therefore based on the equality

$$\mathscr{J} = \mathscr{J}^{\mathrm{c}} \equiv 2\gamma, \tag{65}$$

where γ is called the fracture surface energy. For homogeneous external loading, the equation

$$\mathscr{J} = 2\gamma \tag{66}$$

defines the surface of the second order, in a six-dimensional space, of stresses $\boldsymbol{\sigma}$. In particular, for a penny shaped crack with radius R^{c}, Eqs. (5) and (66) turn into

$$\frac{2(1-\nu)R^{\mathrm{c}}}{\pi\mu}\left(\sigma_{11}^2 + \left[\frac{2}{2-\nu}\right]^2\sigma_{12}^2 + \left[\frac{2(1-\nu)^2}{2-\nu}\right]\sigma_{13}^2\right) = 2\gamma, \tag{67}$$

(see, e.g. Murakami, 1987). Thus, we have obtained the strength criterion Eq. (67) in terms of Eq. (59), in which the strength tensor $\boldsymbol{\Pi}^4$ is a function of the size and orientation of the crack. This analogy permits the use of the strength calculation method of composites developed in Section 8.1.

Let us consider a crack within a statistically homogeneous inclusion field. At first glance, it would seem that it is possible to define the first approximation to an estimated effective energy release rate $\mathscr{J}^*(\mathbf{z})$ by means of SIF

$$\mathscr{J}^*(\mathbf{z}) = \boldsymbol{\Lambda}(\langle\mathbf{K}(\mathbf{z})\rangle \otimes \langle\mathbf{K}(\mathbf{z})\rangle) \equiv \boldsymbol{\Lambda}(\mathbf{K}^0(\mathbf{z}) \otimes \mathbf{K}^0(\mathbf{z})), \tag{68}$$

where the equality follows from Eq. (17) and indicates that the residual stress generated, $\mathscr{J}*(\mathbf{z})$ (at $\boldsymbol{\sigma}^0 \equiv \mathbf{0}$) is very much determined by stress fluctuations in the vicinity of the crack tip.

Use of a conditional SIF is expected to be more correct ($k = 0, 1,...$),

$$\mathscr{J}^*(\mathbf{z}) = \max_k \max_{\mathbf{x}_k} \mathscr{J}(\langle\mathbf{K}(\mathbf{z})|v_k, \mathbf{x}_k\rangle)\langle\gamma\rangle/\gamma^{(k)} = 2\langle\gamma\rangle \tag{69}$$

$$\mathscr{J}(\langle\mathbf{K}(\mathbf{z})|v_k, \mathbf{x}_k\rangle) \equiv \boldsymbol{\Lambda}\big[\langle\mathbf{K}(\mathbf{z})|v_k, \mathbf{x}_k\rangle \otimes \langle\mathbf{K}(\mathbf{z})|v_k, \mathbf{x}_k\rangle\big], \tag{70}$$

where the multiplier $\langle\gamma\rangle$ is introduced for the purpose of preserving the conservation of the dimensionality of $\mathscr{J}^*$. This multiplier is used for the case $\gamma^{(0)} > \gamma^{(\mathrm{i})}$ ($\forall i = 1, 2,..., N$); otherwise the multiplier $\langle\gamma\rangle$ should be replaced by the factor $\langle 1/\gamma\rangle$.

Eq. (69) is based on the concept of the weakest link. The mixture rule can be realized by the use of the total probability formula,

$$\begin{aligned}\mathscr{J}^*(\mathbf{z}) = (1-c)\mathscr{J}(\langle\mathbf{K}(\mathbf{z})|v_0, \mathbf{x}_0\rangle)\langle\gamma\rangle/\gamma^{(0)} + \sum_{m=1}^{N}\langle\gamma\rangle n^{(m)}/\gamma^{(m)} \int \boldsymbol{\Lambda}\langle\mathbf{K}(\mathbf{z})|v_m, \mathbf{x}_m\rangle \\ \otimes \langle\mathbf{K}(\mathbf{z})|v_m, \mathbf{x}_m\rangle V_m^{\mathbf{z}}(\mathbf{x}_m)\mathrm{d}\mathbf{x}_m = 2\langle\gamma\rangle,\end{aligned} \tag{71}$$

where $V_m^{\mathbf{z}}$ designates a characteristic function of the inclusion v_m with the center $\mathbf{z}$; Eq. (70) has been outlined for spherical inclusions and can be used as an approximation in the general case.

However, at this time, we can calculate the second conditional moments of SIF and, therefore, it would appear reasonable that the generalization of Eqs. (69) and (71) is ($k = 0, 1,...$)

$$\mathscr{J}^*(\mathbf{z}) = \max_k \; maxfrom\mathbf{x}_k \langle \mathscr{J}(\mathbf{z})|v_k, \mathbf{x}_k\rangle\langle\gamma\rangle/\gamma^{(k)} = 2\langle\gamma\rangle \tag{72}$$

$$\mathscr{J}^*(\mathbf{z}) = (1-c)\langle \mathscr{J}(\mathbf{z})|v_0, \mathbf{x}_0\rangle\langle\gamma\rangle/\gamma^{(0)} + \sum_{m=1}^{N}\langle\gamma\rangle n^{(k)}/\gamma^{(m)} \int \langle \mathscr{J}(\mathbf{z})|v_m, \mathbf{x}_m\rangle V_m^{\mathbf{z}}(\mathbf{x}_m)\mathrm{d}\mathbf{x}_m = 2\langle\gamma\rangle, \tag{73}$$

respectively, where $k = 0, 1,...,$ and

$$\langle \mathscr{J}(\mathbf{z})|v_k, \mathbf{x}_k\rangle \equiv \mathbf{\Lambda}\langle \mathbf{K}(\mathbf{z}|v_k, \mathbf{x}_k) \otimes \mathbf{K}(\mathbf{z}|v_k, \mathbf{x}_k)\rangle \tag{74}$$

can be found from the formulae for the second stress moment in the vicinity of a crack tip (Eqs. (32) and (36)); in so doing, only the singularity terms proportional to degree -1 in ρ are taken into account in the calculation of $\langle \mathscr{J}(\mathbf{z})|v_k, \mathbf{x}_k\rangle$ because, according to Wilson and Yu (1979), the contribution of terms with the lesser singularity equals zero.

It should be noted that the energy release rate is a nonlinear function of SIF and SIF, in turn, is a random value. A schematic representation of Eqs. (69) and (70) is based on the assumption $\langle \mathscr{J}|v_J, \mathbf{x}_J\rangle = \mathscr{J}(\langle \mathbf{K}|v_J, \mathbf{x}_J\rangle)$ ($J = 0, i$; $i = 1, 2,...$) which produces a large error as the SIF dispersion increases. For analysis of stress fluctuation effects, we will define a fluctuation part of both the expectation and conditional expectation of values of the energy release rate ($J = 0, i$; $i = 1, 2,...$)

$$\Delta\mathscr{J}(\mathbf{z}) \equiv \langle \mathscr{J}(\mathbf{z})\rangle - \mathscr{J}(\langle \mathbf{K}(\mathbf{z})\rangle) \tag{75}$$

$$\Delta\mathscr{J}(\mathbf{z}|v_J, \mathbf{x}_J) \equiv \langle \mathscr{J}(\mathbf{z})|v_J, \mathbf{x}_J\rangle - \mathscr{J}(\langle \mathbf{K}(\mathbf{z})|v_J, \mathbf{x}_J\rangle), \tag{76}$$

where the terms in the right-hand-side of Eq. (76) are determined by Eqs. (74) and (70), respectively. Taking Eq. (68) into account, the second term of the right-hand-side of Eq. (75), $\mathscr{J}(\langle \mathbf{K}(\mathbf{z})\rangle)$ is defined only by the remote stresses: $\mathscr{J}(\langle \mathbf{K}(\mathbf{z})\rangle) = \mathscr{J}(\mathbf{K}^0(\mathbf{z}))$. Moreover, in conformity with the Jensen inequality for the convex function, $\mathscr{J} = \mathscr{J}(\mathbf{K})$, we have the following inequalities: $\Delta\mathscr{J}(\mathbf{z}) \geq 0$ and $\Delta\mathscr{J}(\mathbf{z}|v_J, \mathbf{x}_J) \geq 0$. Here, the equalities take place if and only if the inclusion fields are deterministic.

8.3. Dilute concentration of microcracks

For simplicity's sake, we assume that microcrack concentration is dilute and the interaction between microcracks can be neglected; in principle this reciprocal action can be estimated by use of the multiparticle effective field method (see Buryachenko and Lipanov, 1986a, 1986b; Buryachenko and Kreher, 1995) with some additional hypothesis. We will take into account the stochastic character of the stresses generated by the random inclusion field. Of course, the microcracks may come into being at any location (inside inclusions, the matrix and/or inclusion boundaries); but according to a large body of experimental research (Cutler and Vircar, 1985; Tvergard and Hutchinson, 1988; Luo and Stevens, 1993), the microcracks come into existence at grain faces. For the sake of definiteness, we will assume that the microcracks have a penny-shaped form with $R^{\mathrm{c}} \leq a$ and centered near the inclusion surface. The geometrical microstructure of the composite is taken to be isotropic and, therefore, the microcrack orientation can be selected in an arbitrary way, say, $\mathbf{n} = (1, 0, 0)^{\top}$, with the center $\mathbf{x}$ of an inclusion. The microcrack size is closely connected with the inclusion dimensions and we assume that it is the same as the grain face. Then the microcrack radii R^{c}, expressed by means of inclusion radius a by application of the relation $R^{\mathrm{c}} = 2a/\sqrt{n_{\mathrm{f}}}$ (see Ortiz and Molinari, 1988), where n_{f} is the number of faces per grain and varies between nine and eighteen; for a tetradecahedra, as an example, $n = 14$ and therefore $R^{\mathrm{c}} = 0.53a$.

At first, we consider the microcrack S which is located throughout inside the inclusion $S \subset v_1$. Then,

for estimation of the conditional energy release rate, $\langle \mathscr{J}(\mathbf{z})|v_1,\ \mathbf{x}_1\rangle$, one can use Eq. (73) previously obtained. However, another location of the microcrack is of more practical significance. This is a case when either part of, or the whole microcrack is inside the matrix. For this purpose, it is necessary to evaluate at least the two-point conditional statistical moments of stresses $\sigma(\mathbf{x}|S,\ v_1,\ \mathbf{x}_1;\ v_0,\ \mathbf{x}_0)$, where point $\mathbf{x}_0$ coincides with the point $\mathbf{z}$ of a crack tip Γ^{c}. The relations for the condition average, $\langle\sigma(\mathbf{x}|v_1,\ \mathbf{x}_1;\ v_0,\ \mathbf{x}_0)\rangle$ and for the conditional second moment, $\langle\sigma(\mathbf{x}|S,\ v_1,\ \mathbf{x}_1;\ v_0,\ \mathbf{x}_0)\otimes\sigma(\mathbf{x}|S,\ v_1,\ \mathbf{x}_1;\ v_0,\ \mathbf{x}_0)\rangle$, can be easily found using Eqs. (25) and (36), through the interchange of the binary correlation function $\phi(v_p,\ \mathbf{x}_p|;v_1,\ \mathbf{x}_1)$ with a triple one, $\phi(v_p,\ \mathbf{x}_p|;v_1,\ \mathbf{x}_1;\ v_0,\ \mathbf{x}_0)$. In a like manner, it should present no problem to analyze the situation when the microcrack is located completely inside the matrix near a fixed inclusion.

9. Scheme of simple probability model of composite fracture

The proposed strength and fracture criterion (Eqs. (62), (72), (73) and (74)) are based on the determination of the conditional averages $\langle\mathbf{\Pi}^{(k)}(\boldsymbol{\sigma})\rangle$ and $\langle\mathscr{J}(\mathbf{z})|v_J,\ \mathbf{x}_J\rangle$ ($k = 0, 1,..., N$; $J = 0, i$; $i = 1, 2,...$), respectively. In fracture mechanics, for random loading, another approach is known. One of these methods is based on the calculation of the distribution, $F_Y(y)$, of some fracture parameter Y (see, e.g. Bolotin, 1993). Such a parameter can be identified with different nonlinear functions of local stresses. For example, for $Y=\mathbf{\Pi}^{(k)}(\boldsymbol{\sigma})$ Eq. (59), we have a critical value $y^{\mathrm{crit}}=1$; in a similar manner in fracture mechanics, for $Y=\mathscr{J}(\mathbf{K})$, we have $y^{\mathrm{crit}}=2\gamma$. Thereafter, the first-order estimation of the fraction of fractured component f (or grain faces) is calculated as

$$f = 1 - F_Y(y). \tag{77}$$

Usually, the approach assumes that the damage density is small enough so that the interaction of fractured elements is negligibly small.

For simplicity, the stress distribution within each component is assumed as a six-dimensional Gaussian one, with distribution function $\Phi_{\sigma}^{(k)}(\boldsymbol{\sigma})$, $\boldsymbol{\sigma}=(\sigma_1,...,\ \sigma_6)^{\top}$. Then pertinent damages (or the fracture probability of the component) can be defined by the relation (Bolotin, 1993) ($k = 0, 1,..., N$)

$$f^{(k)} = 1 - \int \mathrm{d}\Phi^{(k)}(\boldsymbol{\sigma}),\ (k = 0, 1, \ldots, N). \tag{78}$$

In a similar manner, the probability of a crack propagating at the point $\mathbf{z}\in\Gamma^{\mathrm{c}}$, located either in the matrix or inclusion v_k ($k = 0, 1,...$) can be calculated as

$$f^{(k)}(\mathbf{z}|v_k,\ \mathbf{x}_k) = 1 - \int \mathrm{d}\Phi^{(k)}(\mathbf{K}|v_k,\ \mathbf{x}_k), \tag{79}$$

where one assumes a three-dimensional Gaussian distribution of SIF with the expectation value $\langle\mathbf{K}(\mathbf{z})|v_k,\ \mathbf{x}_k\rangle$ Eq. (27) and the covariance matrix

$$\Delta\mathbf{K}^2(\mathbf{z}|v_k,\ \mathbf{x}_k) \equiv \langle\mathbf{K}(\mathbf{z}|v_k,\ \mathbf{x}_k)\otimes\mathbf{K}(\mathbf{z}|v_k,\ \mathbf{x}_k)\rangle - \langle\mathbf{K}(\mathbf{z})|v_k,\ \mathbf{x}_k\rangle\otimes\langle\mathbf{K}(\mathbf{z})|v_k,\ \mathbf{x}_k\rangle, \tag{80}$$

which can be found either by Eq. (32) or Eq. (36).

In the right-hand-side integrals of Eqs. (78) and (79), the integral domains are determined by one of two inequalities ($k = 0, 1,..., N$)

$$\mathbf{\Pi}^{(k)}(\boldsymbol{\sigma})\leq 1 \tag{81}$$

for Eq. (78) and

$$\mathbf{\Lambda}^{(k)}(\mathbf{K}\otimes K)\le 2\gamma^{(k)} \text{ or } K_1<0 \tag{82}$$

for Eq. (79). By the use of the second inequality of Eq. (82), we assume the impossibility of fracture under compressive normal loading. The boundaries Eqs. (81) and (82) are described by the surface of the second order in stress space in the simple case of a quadratic strength criterion Eq. (59) and an elliptical plane crack within a homogeneous stress field.

The simplest phenomenological ways of fracture probability calculation for composites (Sobczuk and Spencer, 1991) are based either on the total probability formula,

$$f=\sum_{k=0}^{N} c^{(k)}f^{(k)}, \tag{83}$$

or the extreme value distribution,

$$f=1-\prod_{k=0}^{N}(1-f^{(k)}). \tag{84}$$

Ortiz and Molinari (1988) were the first to consider the particular case of this scheme with an application to random structure composites. By the use of Fourier's method, they obtained the estimation for the second moment of stresses averaging over all volume of a composite with elastically homogeneous properties, but with stress-free strain fluctuations. Because the residual stresses are self equilibrating, we have $\delta\boldsymbol{\sigma}\equiv\boldsymbol{\sigma}-\langle\boldsymbol{\sigma}\rangle=\boldsymbol{\sigma}$. Thereupon, Ortiz and Molinari (1988), and Ma and Clarke (1994) have assumed that the residual stresses are normally distributed with a zero expectation in each point of the composite. Slight modification of this approach takes into account the average stresses in the components, which can be estimated by using the exact Eq. (29). Therefore, the definition of the conditional covariance matrix and probability density function and probability density function are defined by the formulae (see, for details, Buryachenko and Rammerstorfer, 1998)

$$K^{\sigma(i)}_{klmn}=\langle\sigma_{kl}\sigma_{mn}\rangle_i(\mathbf{x})-\langle\sigma_{kl}\rangle_i\langle\sigma_{mn}\rangle_i, \tag{85}$$

$$\mathrm{d}\Phi^i_\sigma(\delta\sigma)=\frac{1}{\sqrt{(2\pi)^N\det\mathbf{K}^{\sigma(i)}}}\exp\left[-\frac{1}{2}(\sigma_{kl}-\langle\sigma_{kl}\rangle_i)(K^{\sigma})^{-1}_{klmn}(\sigma_{mn}-\langle\sigma_{mn}\rangle_i)\right]. \tag{86}$$

10. Numerical results

10.1. The first and the second statistical moments of stress intensity factors

As an example, we consider a Si_3N_4 composite with isotropic components $\mathbf{L}(\mathbf{x})=(3k,\ 2\mu)\equiv 3k\mathbf{N}_1+2\mu\mathbf{N}_2$, $\boldsymbol{\beta}_1=\beta_{10}\boldsymbol{\delta}$, $\mathbf{N}_1\equiv\boldsymbol{\delta}\otimes\boldsymbol{\delta}/3$ and $\mathbf{N}_2\equiv\mathbf{I}-\mathbf{N}_1$, containing identical SiC spherical inclusions. Based on the results of Buryachenko (1999b), we assume an elastically homogeneous medium with the elastic properties of the matrix $k=236.4$ GPa, $\mu=121.9$ GPa (Young's modulus $E=312.1$ GPa, Poisson's ratio $\nu=0.28$), $\beta_{10}=-1\times10^{-3}$ and the radius of the inclusions $a=10^{-5}$ m. For the representation of numerical results in dimensionless form, we define the normalizing coefficient $\vartheta\equiv-3Q^k\beta_{10}\sqrt{a}$, where $3Q^k$ equals the bulk component of the tensor $\mathbf{Q}_i=(3Q^k,\ 2Q^\mu)$. The physical meaning of ϑ follows from Eq. (23), according to which, ϑ varies proportionally with the component of hydrostatic stress inside a

single isolated inclusion in an infinite homogeneous matrix; for our concrete composite SiC/Si_3N_4: $\vartheta = 0.914$ MPa m^{-2}. We will estimate the action of the alternative radial distribution function for an inclusion ($r \equiv |\mathbf{x}_i - \mathbf{x}_j|$)

$$g(\mathbf{x}_i - \mathbf{x}_j) \equiv \phi(v_i, \mathbf{x}_i|; v_j, \mathbf{x}_j)/n_i = H(r - 2a) \tag{87}$$

and (see Eq. 7.2 in Buryachenko, 1999b),

$$g(\mathbf{x}_i - \mathbf{x}_j) = H(r - 2a)\left\{1 + \left[\frac{2 + c}{2(1 - c)^2} - 1\right]\cos\left(\frac{\pi r}{a}\right)\right\}\mathrm{e}^{2(2 - r/a)}. \tag{88}$$

In order to carry out the numerical estimates, we will use the expressions of the tensors $\mathbf{Q}_p$, $\mathbf{T}_p(\mathbf{x} - \mathbf{x}_p)$ ($p = 1, 2, \ldots$), which are presented e.g. by Buryachenko and Rammerstorfer (1997).

At first, we consider one fixed inclusion v_1 with the center $\boldsymbol{x}_1 = (0, R^c + r, 0)$ near the crack tip $\mathbf{z} = (0, R^c, 0) \in \boldsymbol{\Gamma}^c$, $S \perp \mathbf{n} = (1, 0, 0)$, and $\boldsymbol{\sigma}^0 \equiv \mathbf{0}$. Fig. 1 shows the residual stress generated normalized mode I SIF $K_I^1(\mathbf{z}, v_1, \mathbf{x}_1)/\vartheta$ as a function of the normalized distance r/a from the inclusion center $\mathbf{x}_1 = (0, R^c + r, 0)$ to the crack tip $\mathbf{z}$, for the different relative sizes of the crack $R^c = 1000a$, $R^c = 10a$ and $R^c = 3a$. It can be seen from Fig. 1 that the variation between the calculated values, $K_I^1(\mathbf{z}, v_1, \mathbf{x}_1)/\vartheta$, is not more than 4% for $R^c = 1000a$ and $R^c = 3a$ under $|r| < a$; for $R^c = 1000a$ and $R^c = 10a$, this quantity is less than 2% $\forall r$. Therefore, for $R^c > 10a$, the crack may be considered as a semi-infinite crack; in the following, unless otherwise specified, we will consider the case $R^c = 100a$. It is interesting that if the inclusion is located in the point $r/a \cong 0.93$ (as read approximately from the graphs), it does not initiate a stress singularity near crack tip $K_I^1(\mathbf{z}, v_1, \mathbf{x}_1) = 0$ (in view of the problem symmetry, $K_{II}^1(\mathbf{z}, v_1, \mathbf{x}_1) = K_{III}^1(\mathbf{z}, v_1, \mathbf{x}_1) \equiv 0\ \forall r$). Hereafter, instances of negative $K_I^1(\mathbf{z}, v_1, \mathbf{x}_1) = 0$ are simply numerical results related to the compression, and have no physical meaning in the sense of material overlap or penetration. The addition of a remote loading generating $K_I^0(\mathbf{z})$ will increase the total stress intensity factor, $K_I(\mathbf{z}, v_1, \mathbf{x}_1) = K_I^0(\mathbf{z}) + K_I^1(\mathbf{z}, v_1, \mathbf{x}_1)$, as stated previously. If in so doing, $K_I(\mathbf{z}, v_1, \mathbf{x}_1) > 0$, then the negative residual stress generated SIF $K_I^1(\mathbf{z}, v_1, \mathbf{x}_1)$ has a physical meaning of the shielding (or unloading) effect. For example, at the spacing $r/a < -1$, the crack-inclusion interaction results in shielding: $K_I(\mathbf{z}, v_1, \mathbf{x}_1) < K_I^0(\mathbf{z})$. The impact of the inclusion on the crack is highly localized in the region $|r| < 2a$ and rapidly becomes negligible at the

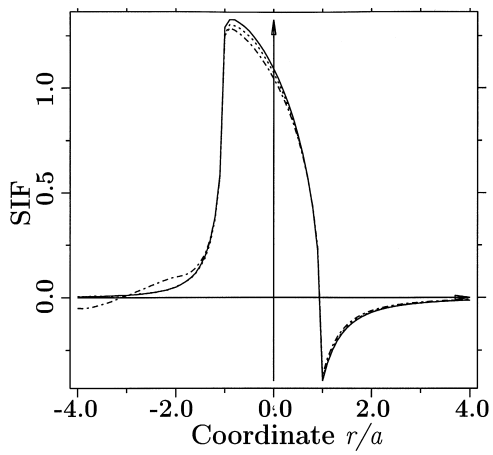

Fig. 1. Normalized modes I SIF $K_I^1(\mathbf{z}, v_1, \mathbf{x}_1)/\vartheta$ as a function of inclusion localization r for different crack sizes $R^c = 1000a$ (solid curve), $R^c = 10a$ (dotted curve), and $R^c = 3a$ (dot–dashed curve).

further points. This indicates that, in the case of a crack interacting with many inclusions, we can expect a short-range interaction effect. This seems to imply that the size of the so-called representative volume element (RVE) will be small enough.

In order to illustrate the method and to examine the influence of the spatial arrangement of the inclusions, we come now to the evaluation of conditional averages $\langle \mathbf{K}^1(\mathbf{z})|v_J, \mathbf{x}_J\rangle$ ($J = 0,1$) Eq. (28). For the fixed inclusion, the normalized curves $\langle K_{\mathrm{I}}^1(\mathbf{z})|v_1, \mathbf{x}_1\rangle/\vartheta$ are calculated in Fig. 2. by the use of the step radial distribution function Eq. (87) and the real one Eq. (88) for $c = 0.4$. For the matrix located in the point $\mathbf{x}_0 = (0, R^{\mathrm{c}} + r, 0)$, the relevant curve is calculated under the step correlation function,

$$\phi(v_p, \mathbf{x}_p|; v_0, \mathbf{x}_0) = H(|\mathbf{x}_p - \mathbf{x}_0| - a)n^{(1)}. \tag{89}$$

Notwithstanding the fact that the conditional average stresses inside each component in the absence of a crack $\langle \boldsymbol{\sigma}^{\mathrm{ac}}\rangle_1$ Eq. (29) and $\langle \boldsymbol{\sigma}^{\mathrm{ac}}\rangle_0$ Eq. (30) do not depend on the radial distribution function g, it is evident from Fig. 2 that the significant influence of neighboring order in localization of the inclusions on the values of $\langle K_{\mathrm{I}}^1(\mathbf{z})|v_J, \mathbf{x}_J\rangle/\vartheta$ ($J = 0, 1$). Such strong influence of g on the conditional average SIF is explained by the essentially nonlinear dependence of SIF on the local stresses near the crack tip. Moreover, the perturbation generated by surrounding inclusions $\langle K(\mathbf{z})|v_i, x_i\rangle - K(\mathbf{z}, v_i, x_i)$ is a linear function of the inclusion concentration for the step radial function Eq. (87). Therefore, the normalized curve, $[\langle K_{\mathrm{I}}^1(\mathbf{z})|v_i, \mathbf{x}_i\rangle - K_{\mathrm{I}}^1(\mathbf{z}, v_i, \mathbf{x}_i)]/\vartheta c$, is a weak function of ν and varies by 1%, at most, for the range of values $0.2 \le \nu \le 0.4$. In this connection, it should be mentioned that the analogous two-dimensional model representation of a two-component material containing randomly fluctuating residual stresses was analyzed by Lipetzky and Kreher (1994) by the use of the Monte Carlo simulations of the microstructure with a wide distribution of inclusion sizes. For $c = 0.3$ and a single case of the fixed inclusion v_1 with center $\mathbf{x}_1 = (0, R^{\mathrm{c}} + a, 0)$, they evaluated $\langle K_{\mathrm{II}}^1(\mathbf{z})|v_1, \mathbf{x}_1\rangle = 0$ and $\langle K_{\mathrm{I}}^1(\mathbf{z})|v_1, \mathbf{x}_1\rangle = -0.5\ \mathrm{MPa\,m^{-2}}$, in conformity with Fig. 2: $\langle K_{\mathrm{I}}^1(z)|v_1, \mathbf{x}_1\rangle = -0.7\ \mathrm{MPa\,m^{-2}}$.

The curves plotted in Fig. 2 depend on g and ν, and are invariant with respect to both another thermo-elastic properties of components and the size of inclusions as well. From Fig. 2, we see that the conditional average, $\langle K_{\mathrm{I}}(\mathbf{z})|v_0, x_0\rangle$, under the condition of the location in the matrix at the point $\mathbf{x}_0 = (0, R^{\mathrm{c}} + r, 0)$ is less with respect to the magnitude than the average $\langle K_{\mathrm{I}}(\mathbf{z})|v_1, \mathbf{x}_1\rangle$ with fixed inclusion in the

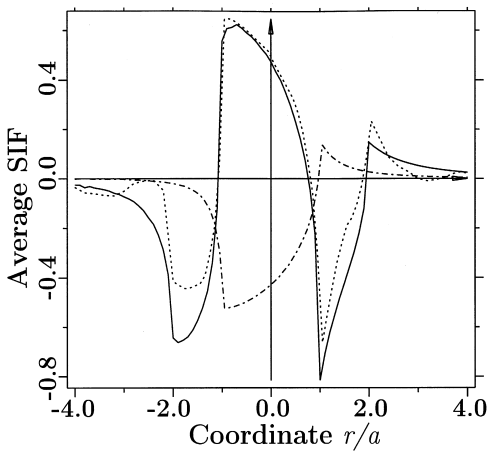

Fig. 2. Conditional normalized averages $\langle K_{\mathrm{I}}^1(\mathbf{z})|v_1, \mathbf{x}_1\rangle/\vartheta$ (solid and dotted curves) and $\langle K_{\mathrm{I}}^1(\mathbf{z})|v_0, \mathbf{x}_0\rangle/\vartheta$ (dot–dashed curve) calculated for either the real correlation function Eq. (88) (dotted curve) and the step function Eq. (87) (solid and dot–dashed curve).

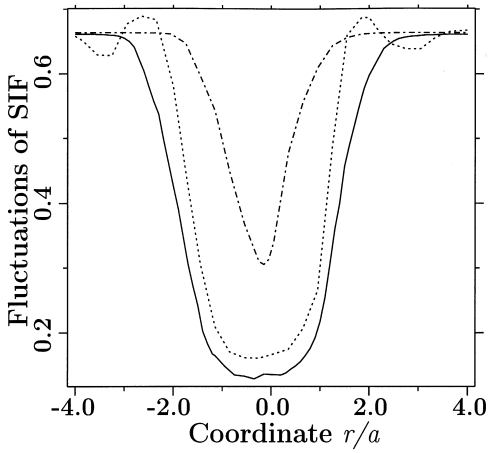

Fig. 3. Normalized SIF fluctuation of mode I $[\Delta K_{\rm I}^1(\mathbf{z}|v_k,\mathbf{x}_k)]^{1/2}/\vartheta$ as a function of either an inclusion location (solid and dotted curves, $k = 1$) and the matrix location (dot–dashed curve, $k = 0$) calculated for either the real correlation function Eq. (88) (dotted curve) and the step function (Eqs. (87) and (89)) (solid and dot–dashed curve, respectively).

point $\mathbf{x}_1 = (0,\ R^{\rm c}+r,\ 0)$. It turns out that the relative placement of the curves for the SIF fluctuations $\Delta\mathbf{K}^2(\mathbf{z}|v_k,\ \mathbf{x}_k) \equiv \langle\mathbf{K}^2(\mathbf{z})|v_k,\ \mathbf{x}_k\rangle - \langle\mathbf{K}(\mathbf{z})|v_k,\ \mathbf{x}_k\rangle^2$ ($k = 0,1$) is interchanged.

For zero remote loading ($\boldsymbol{\sigma}^0 \equiv \mathbf{0}$) in Figs. 3 and 4, the normalized curves $[\Delta K_i^2(\mathbf{z}|v_k,\ \mathbf{x}_k)]^{1/2}/\vartheta \sim r/a$ (i = I, II; $k = 0,1$) are plotted for the step radial function Eq. (87) and the real one Eq. (88) (the similar results take place for i = III, $k = 0, 1$). Analogous results for the matrix located in the point $\mathbf{x}_0 = (0,\ R^{\rm c}+r,\ 0)$ represent for the case of a step correlation function Eq. (89) only. We see that the fluctuation of the mode II SIF (and the mode III SIF as well) are not equal to zero, although there is a symmetry of the problem being analyzed and, therefore, $\langle K_{\rm II}^1(\mathbf{z}|v_k,\ \mathbf{x}_k)\rangle = \langle K_{\rm III}^1(\mathbf{z}|v_k,\ \mathbf{x}_k)\rangle \equiv \mathbf{0}$ at $\boldsymbol{\sigma} = 0$. It is clear that the reason why the conditional fluctuations of the SIF under matrix cracks are materially greater than fluctuations of the SIF with the fixed inclusion. Really, these values defined by the action of surrounding inclusions v_p (p = 2, 3,...), but the distances from the center $\mathbf{x}_p$ of the nearest inclusion v_p

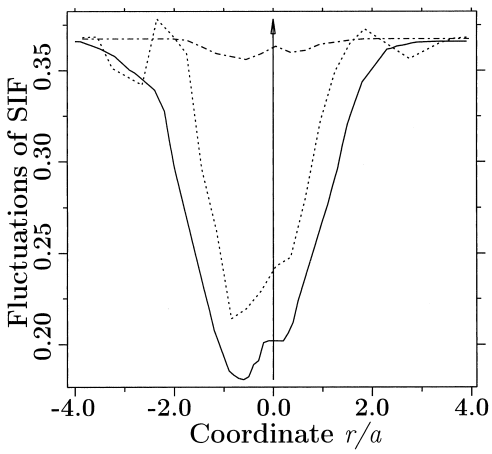

Fig. 4. Normalized SIF fluctuation of mode II $[\Delta K_{\rm II}^1(\mathbf{z}|v_k,\mathbf{x}_k)]^{1/2}/\vartheta$ (the notation of Fig. 3).

(p = 2, 3,...) to the fixed point $\mathbf{x}_J$ (J = 0, 1) are differ among themselves: $|\mathbf{x}_p-\mathbf{x}_1|=2|\mathbf{x}_p-\mathbf{x}_0|$. The minimum of $\Delta K_i^2(\mathbf{z}|v_J, \mathbf{x}_J)$ (i = I, II, III; J = 0, 1) occurs for the location of the fixed point near a crack tip $\mathbf{z}$. For the remote field points, $\mathbf{K}^2(\mathbf{z}|v_J, \mathbf{x}_J) \to$ const. $\neq \mathbf{0}$ under $|\mathbf{x}_J-\mathbf{z}| \to \infty$ (J = 0, 1). For the step radial functions Eq. (57) $\Delta\mathbf{K}^2(\mathbf{z}|v_J, \mathbf{x}_J)/c$ does not depend on the inclusion concentration. Recall that because the crack size is constant and at the estimation of $\langle\mathbf{K}^1(\mathbf{z})|v_J, \mathbf{x}_J\rangle$, the influence of the remote loading equals zero, the randomness of the stress intensity factor is not a result of any intervention by an external effect, but rather a direct result of the many possible residual stress states. As a consequence, the fluctuations of SIFs $\Delta\mathbf{K}^2(\mathbf{z}) \neq \mathbf{0}$, in spite of the exact results $\langle\mathbf{K}(\mathbf{z})\rangle \equiv \mathbf{K}^0(\mathbf{z})$, as well as $\langle\mathbf{K}(\mathbf{z})\rangle \equiv \mathbf{0}$ at $\boldsymbol{\sigma}^0 \equiv \mathbf{0}$.

Let us consider the crack tip inside a finite random cloud of inclusions. For the sake of definiteness, the cloud being analyzed has a form of a ball with center $\mathbf{x}^{\text{fin}}=(0, R^{\text{c}}+r^{\text{fin}}, 0)$ and radius a^{fin}; inclusion concentration equals a constant in the cloud $\phi(v_i, \mathbf{x}_i)=c$, $\mathbf{x}_i \in v^{\text{fin}}$. Then $\langle\mathbf{K}(\mathbf{z})\rangle$ may be estimated by the use of Fig. 1, by replacing a, $\mathbf{x}_1$ and $\boldsymbol{\beta}_{10}$ by a^{fin}, $\mathbf{x}^{\text{fin}}$ and $c\boldsymbol{\beta}_{10}$, respectively. It is easy to perceive that, for a sufficiently large cloud, in general $|\langle\mathbf{K}(\mathbf{z})\rangle| \gg |\langle\mathbf{K}(\mathbf{z})|v_1, \mathbf{x}_1\rangle^{\text{inf}}|$ $\forall\mathbf{x}_i$ and the SIF fluctuations are negligibly small quantities compared with $\langle\mathbf{K}(\mathbf{z})\rangle$. But from Fig. 1, we notice that there is a point $r^{\text{fin}} \cong 0.93a^{\text{fin}}$, for which $\langle\mathbf{K}(\mathbf{z})\rangle=\mathbf{0}$ and the conditional averages and the fluctuations formally coincide with the analogous values found for the infinite random field of the inclusions, see Eqs. (54) and (55).

It should be mentioned that Figs. 1–4 were plotted in the dimensionless form by the use of the normalized coefficient ϑ. The curves obtained above depend only on Poisson's ratio ν and are invariants with respect to both the other thermoelastic properties of the components and the inclusion size. But for the range of values $0.2 \leq \nu \leq 0.4$, the calculated curves for both the conditional averages and fluctuations of SIF vary 0.5% at most for mode I and 4% for modes II and III. For $0.05 \leq \nu \leq 0.49$, the normalized values may differ by 10%. In so doing, the stress fluctuation $[\Delta\boldsymbol{\sigma}_k^2(\mathbf{x})]^{1/2}/\vartheta$ (k = 0, 1) can vary even more drastically (see Buryachenko, 1999b). It seems difficult to justify such small variations of the normalized conditional averages of SIF and SIF fluctuations inside the practically important range $0.2 \leq \nu \leq 0.4$. But it is because of this fact that such figures may be used for analysis of the wide class of elastically homogeneous composites with the microtopology of transformed inclusions studied here.

10.2. Effective energy release rate

For representation of the numerical estimations of $\langle\mathscr{J}(\mathbf{z})|v_J, \mathbf{x}_J\rangle$ and $\Delta\mathscr{J}(\mathbf{z}|v_J, \mathbf{x}_J)$ (J = 0, i; i = 1, 2,...) in dimensionless form, we define the normalized coefficient $\theta \equiv (1-\nu)\vartheta^2/(2\mu)$ and a dimensionless parameter $\xi=2\gamma/\theta$, where ν is a Poisson's ratio. According to Eqs. (23) and (67), the coefficient θ is proportional to the energy release rate for a single penny-shaped microcrack with radius $R^{\text{c}}=a$ within an isolated spherical inclusion in the infinite homogeneous matrix. For example, in line with Section 10.1 the composite material Si_3N_4–SiC with SiC spherical inclusions may be considered as an elastically homogeneous material with the parameters k = 236.4 GPa, $\mu=121.9$ GPa, $\beta_{10}=-10^{-3}$, $a=10^{-5}$ m, $\gamma(\mathbf{x}) \equiv \gamma=7\times10^{-2}$ MPa m; therefore, in this concrete case $\theta=2.47\times10^{-6}$ MPa m, $\xi=5.67\times10^4$.

Below, the numerical estimations for different average energy release rates will be obtained in the form of normalized curves by the use of coefficient θ. These curves are defined only by microtopology of the material and have a weak dependence on ν. We will represent the calculation only for $\nu=0.28$ (composite Si_3N_4–SiC) and will estimate the boundaries of its variation under the change of ν. Similarly, the fracture probability of composite will be represented as a function of ξ, depending on the material microtopology and Poisson's ratio. For simplicity's sake, only the binary interaction of the inclusions will be taken into account.

At first, we analyze $\mathscr{J}(\langle\mathbf{K}(\mathbf{z})|v_k, \mathbf{x}_k\rangle)$ (k = 1, 0; $\boldsymbol{\sigma}^0 \equiv \mathbf{0}$) Eq. (69) as a function of the location of either the inclusion (k = 1) or the matrix (k = 0) at the point $\mathbf{x}_k=(0, R^{\text{c}}+r, 0)$. As a consequence of problem symmetry, $\langle K_{\text{II}}^1(\mathbf{z})|v_k, \mathbf{x}_k\rangle = \langle K_{\text{III}}^1(\mathbf{z})|v_k, \mathbf{x}_k\rangle \equiv 0$ $\forall\mathbf{x}_k=(0, R^{\text{c}}+r, 0)$ (k = 0, 1) and, therefore, $\mathscr{J}(\langle\mathbf{K}(\mathbf{z})|v_k,$

$\mathbf{x}_k\rangle) \equiv \mathscr{J}(\langle \mathbf{K_I}(\mathbf{z})|v_k,\ \mathbf{x}_k\rangle)$ is defined only by mode I SIF. Then, for example, at $r/a < -1$, we have $\langle K_{\mathrm{I}}^1(\mathbf{z})|v_1\mathbf{x}_1\rangle < 0$ (see Fig. 2) and the location of the inclusion leads to the reduction of $\mathscr{J}(\langle K(\mathbf{z})|v_1,\ \mathbf{x}_1\rangle)$ (shielding effect). The curves calculated for $\nu = 0.28$ vary in value no greater than 1%, according to the changes in ν through a range $0.05 \le \nu \le 0.49$.

We are coming now to the estimation of the fluctuation part of the conditional average energy release rate $\Delta\mathscr{J}(\mathbf{z}|v_J,\ \mathbf{x}_J)$ ($J = 0,\ i;\ i = 1, 2,...$) Eq. (76). In Fig. 5, the curve $\Delta\mathscr{J}(\mathbf{z}|v_0,\ \mathbf{x}_0)/\theta$ is calculated for the location of the matrix in the point $\mathbf{x}_0$ under the step correlation function Eq. (89) and $c = 0.4$. In the case of the fixed inclusion, the relevant curves are obtained for the distribution function (Eqs. (88) and (87)), respectively. From Fig. 5, we notice that the fluctuating component of $\Delta\mathscr{J}(\mathbf{z}|v_k,\ \mathbf{x}_k)/\theta$ for the localized matrix ($k = 0$) in excess of the fixed inclusion ($k = 1$). For the case of binary interaction of inclusions $\Delta\mathscr{J}(\mathbf{z}|v_k,\ \mathbf{x}_k)/\theta$ ($k = 0,\ 1$) is a linear function of the inclusion concentration c if the step correlation functions (Eqs. (87) and (89)) are used.

It is of interest to estimate the comparative contribution of the normal $\Delta\mathscr{J}^{\mathrm{no}}(\mathbf{z}|v_k,\ \mathbf{x}_k)$ and shear $\Delta\mathscr{J}^{\mathrm{sh}}(\mathbf{z}|v_k,\ \mathbf{x})$ stress fluctuation to $\Delta\mathscr{J}(\mathbf{z}|v_k,\ \mathbf{x}_k) \equiv \Delta\mathscr{J}^{\mathrm{no}}(\mathbf{z}|v_k,\ \mathbf{x}_k) + \Delta\mathscr{J}^{\mathrm{sh}}(\mathbf{z}|v_k,\ \mathbf{x}_k)$. From Fig. 6, it is seen that the normal component $\Delta\mathscr{J}^{\mathrm{no}}(\mathbf{z}|v_k,\ \mathbf{x}_k)/\theta$ is congruent with the shear component $\Delta\mathscr{J}^{\mathrm{sh}}(\mathbf{z}|v_k,\ \mathbf{x}_k)/\theta$, for the case of the step radial functions, Eq. (87) ($k = 1$) and Eq. (89) ($k = 0$). Moreover, $\Delta\mathscr{J}^{\mathrm{sh}}(\mathbf{z}|v_k,\ \mathbf{x}_k) > \Delta\mathscr{J}^{\mathrm{no}}(\mathbf{z}|v_k,\ \mathbf{x}_k)$ over the regions $-1 < r/a < 1$ ($k = 1$) and $r = 0$ ($k = 0$), which arouses considerable interest in actual practice. The curves plotted for $\nu = 0.28$ vary in value no greater than 0.5% for the normal components and 4% for the shear components, according to changes in ν through a range $0.2 \le \nu \le 0.4$; the curves calculated exchange places within $0.05 \le \nu \le 0.49$ by, at most, 1% and 10%, respectively.

Now let us consider a microcrack near and inside a fixed inclusion for the step correlation function Eq. (87) and $c = 0.4$. We assume that crack tip $\mathbf{z}$ is inside the the matrix if $\mathbf{z}$ lies outside the fixed inclusion v_1. We analyze the location of the the inclusion v_1 with center $\mathbf{x}_1 = (0,\ R^{\mathrm{c}} - a + r,\ 0)^{\top}$ near the microcrack $S \perp \mathbf{n} = (1,\ 0,\ 0)^{\top}$ with center $R^{\mathrm{c}} \le a$ and center $\mathbf{x}^{\mathrm{c}} = (0,\ 0,\ 0)^{\top}$; other arrangements of the inclusion v_1 near the microcrack can be considered in a similar manner. The value $r = 0$ corresponds to the case when the crack tip $\mathbf{z}$ belongs to the inclusion boundary. The curves $\langle\mathscr{J}(\mathbf{z}|v_1,\ \mathbf{x}_1)\rangle/\theta$ and $\mathscr{J}(\langle K(\mathbf{z})|v_1,\ \mathbf{x}_1\rangle)/\theta$ are plotted in Fig. 7 for different sizes of microcracks $R^{\mathrm{c}} = a$ and $R^{\mathrm{c}} = 0.53a$. It can be seen that the values of $\langle\mathscr{J}(\mathbf{z}|v_1,\ \mathbf{x}_1\rangle$ vary slightly inside the region $0 < r < 2a$ until the crack tip intersects

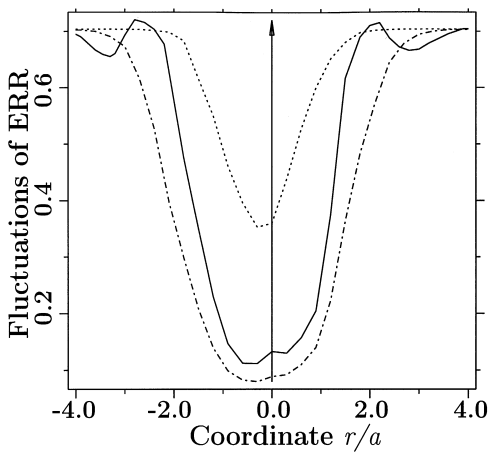

Fig. 5. Fluctuation part of the conditional average of the energy release rate $\Delta\mathscr{J}(\mathbf{z}|v_k,\ \mathbf{x}_k)/\theta$ under fixed matrix (dotted line, $k = 0$) and fixed inclusion for real distribution function Eq. (88) (solid line, $k = 1$) and step one Eq. (87) (dot–dashed line, $k = 1$).

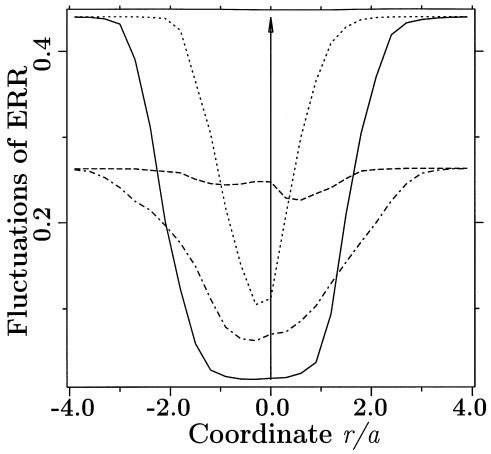

Fig. 6. Normal $\Delta\mathscr{J}^{\mathrm{no}}(\mathbf{z}|v_k,\ \mathbf{x}_k)/\theta$ (solid and dotted lines) and shear $\Delta\mathscr{J}^{\mathrm{sh}}(\mathbf{z}|v_k,\ \mathbf{x})/\theta$ (dashed and dot–dashed lines) components of energy release rate $\Delta\mathscr{J}(\mathbf{z}|v_1,\ \mathbf{x}_1)/\theta$ for fixed matrix (dotted and dashed lines) and inclusions (solid and dot–dashed lines).

the inclusion boundary; thereafter, $\langle\mathscr{J}(\mathbf{z}|v_1,\ \mathbf{x}_1\rangle$ (determined primarily by the mode I SIF) will decrease rapidly. In the example considered, we obtain $\langle K_{\mathrm{I}}(\mathbf{z})|v_1,\ \mathbf{x}_1\rangle < 0$ within the regions $r < -0.06a$ ($R^{\mathrm{c}}=0.53a$) and $r < -0.11a$ ($R^{\mathrm{c}}=a$). Therefore, the values of the energy release rate have no physical meaning inside the regions indicated. As one may have expected, smaller values of $\langle\mathscr{J}(\mathbf{z}|v_1,\ \mathbf{x}_1\rangle$ correspond to smaller microcracks $R^{\mathrm{c}}=0.53a$ (scale effect).

We turn our attention to the prediction of fracture probability of separate components near macrocrack $S\perp\mathbf{n}=(1,\ 0,\ 0)^{\top}$ with radius $R^{\mathrm{c}}=100a$ and center $\mathbf{x}^{\mathrm{c}}=(0,\ 0,\ 0)$ under $c = 0.4$ and the step radial function Eq. (87). In view of the large expenditure of computational time for the case of a fixed inclusion, we will consider only the point $\mathbf{x}_1=(0,\ R^{\mathrm{c}}-0.7a,\ 0)^{\top}$ with maximum conditional SIF $\langle K_{\mathrm{I}}^1(\mathbf{z})|v_1,\ \mathbf{x}_1\rangle = \max$, taking into account that SIF fluctuation is a weak function of $\mathbf{x}_1$ under $|\mathbf{x}_1| < a$. We assume a Gaussian distribution of SIF with conditional average $\langle\mathbf{K}(\mathbf{z})|v_k,\ \mathbf{x}_k\rangle$ ($k = 0,\ 1$) Eq. (27) and

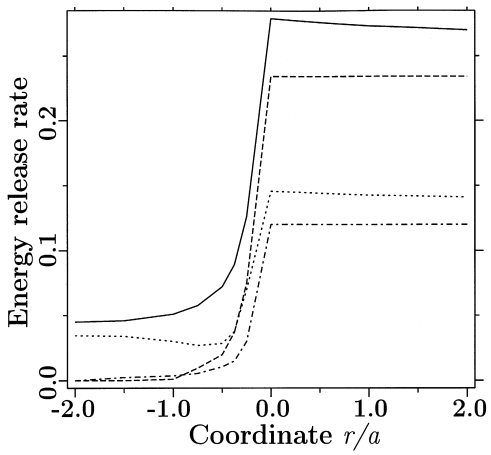

Fig. 7. Total $\langle\mathscr{J}(\mathbf{z})|v_1,\ \mathbf{x}_1\rangle/\theta$ (solid and dotted curves) and a mean part $\mathscr{J}(\langle\mathbf{K}^1(\mathbf{z})|v_1,\ \mathbf{x}_1\rangle)/\theta$ (dashed and dot–dashed curves) of the energy release rate as a function of the inclusion location r/a for: $R^{\mathrm{c}}=a$ (solid and dashed curves) and $R^{\mathrm{c}}=0.53a$ (dot and dot–dashed curves, respectively).

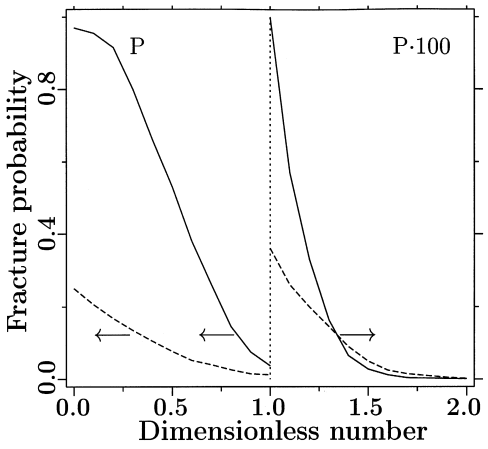

Fig. 8. Fracture probability $P \equiv f^{(k)}(\mathbf{z}, v_k, \mathbf{x}_k)$ ($k = 0, 1$) as a function of dimensionless number ξ for located inclusions in the point of maximum conditional average SIF (solid line) and for fixed matrix (dashed line).

the covariance matrix Eq. (80), which has diagonal form for our case being analyzed. The integration domain in Eq. (79) (the region of safe loading) constitutes the union of an ellipsoidal domain and a half-space Eq. (82). Fig. 8 shows the plots of fracture probability $f^{(k)}(\mathbf{z}|v_k, \mathbf{x})$ (Eqs. (79) and (82)) (for $k = 1$ and for $k = 0$) as a function of the dimensionless number ξ for $c = 0.4$ and step conditional probability densities (Eqs. (87) and (89)). At first glance, it would seem strange that for a sufficiently strong material, $\xi > 1.36$ the fracture probability of the matrix is more than the fracture probability of the inclusion, notwithstanding the fact that $\langle K_{\mathrm{I}}(\mathbf{z})|v_1, \mathbf{x}_1\rangle > 0 > \langle K_{\mathrm{I}}(\mathbf{z})|v_0, \mathbf{x}_0\rangle$. Such a result stands clear when one takes into account the greater level of the SIF fluctuation inside the matrix (see Fig. 2). Therefore, the fracture probability will be fundamentally determined by the maximum SIF fluctuations (other than the conditional average SIF) over the region $\xi \gg 1$, which arouses considerable interest in actual practice. For zero strength of the materials, $f^{(k)}(\mathbf{z}|v_k, \mathbf{x}_k) \to 1 - P\{K_{\mathrm{I}}(\mathbf{z}|v_k, \mathbf{x}_k) < 0\}$ and $f^{(1)}(\mathbf{z}|v_1, \mathbf{x}_1) \to 0.97$, $f^{(0)}(\mathbf{z}|v_0, \mathbf{x}_0) \to 0.28$, which correlates well with our simplifying assumption that the material will not fail under compression.

It is interesting to compare the numerical results just obtained by the use of a probabilistic model with a deterministic model of fracture Eq. (66) near the macrocrack tip ($R^{\mathrm{c}} = 100a$) $\langle \mathscr{J}(\mathbf{z})|v_k, \mathbf{x}_k\rangle = 2\gamma$, when the unit probability of the fracture occurs at $\xi \leq 0.25$ ($k = 1$) and $\xi \leq 0.50$ ($k = 0$). With the use of the conditional average SIF Eq. (70), one should expect fracture of the inclusion at $\xi \leq 0.12$, while fracture of the matrix is impossible. We see that the estimation of fracture probability may be defined more exactly by the application of a more correct model Eq. (68).

It should be noted that all these values of ξ are significantly below the quantity $\xi = 5.67 \times 10^4$ for the Si_3N_4–SiC composite; therefore, internal thermal stresses alone can not break down this specific composite. In the case of additional action of external loading, the stress fluctuation can involve decreasing the level of fracture loading (see, as an example, Lipetzky and Kreher, 1994), but the consideration of this problem is beyond the scope of the present article.

11. Conclusion

The proposed analytical–numerical method is efficient from a computational standpoint and provides a high-accuracy estimation of the energy release rate of a penny-shaped crack in the random field of an

ellipsoidal inclusions with stress-free strains. We show the fundamental role of residual stress fluctuations in the fracture mechanics of composite materials. However, it should be mentioned than actual crack growth is more complicated than simply finding an extreme fluctuation along the crack front, and spatial correlations of stress fields along the crack perimeter come into play here. Furthermore, the numerical results are presented for statistically homogeneous media and the case of graded materials (as well as a boundary value problem), when the concentration of inclusions depends on the coordinates, is not considered. These effects can be estimated by the method proposed and will be pursued in forthcoming papers by the author.

Acknowledgements

Parts of this work were supported by the Max–Planck-Society of Germany and by the Air Force Office of Scientific Research of USA. The author expresses his sincere appreciation to Dr. N.J. Pagano for fruitful discussions and to Ms. E. Gavrilova for preparation of the manuscript.

Appendix A. Integral representations for SIF

The magnitudes of the the modes I, II and III SIFs K_j (j = 1, 2, 3) at the given point $\mathbf{z}=(0,\ R^{\mathrm{c}}\cos\varphi,\ R^{\mathrm{c}}\sin\varphi)^{\top}$ along the front of a crack of radius R^{c} due to an arbitrary distribution of the normal traction $p(\rho_0,\ \varphi_0)$ and the shear one $\tau(\rho_0,\ \varphi_0)$ (arbitrary inclined to the y- and z-axes: $\tau=\tau_x+i\tau_y$) are given by the formulae (Fabrikant, 1989)

$$K_1(\mathbf{z})=\frac{1}{\pi\sqrt{\pi R^{\mathrm{c}}}}\int_0^{2\pi}\int_0^{R^{\mathrm{c}}}\sqrt{R^{\mathrm{c}}2-\rho_0^2}\,\frac{p(\rho_0,\ \varphi_0)\rho_0}{R^{\mathrm{c}}2+\rho_0^2-2R^{\mathrm{c}}\cos(\varphi-\varphi_0)}\,\mathrm{d}\rho_0\,\mathrm{d}\varphi_0$$

$$K_2(\mathbf{z})+iK_3(\mathbf{z})=\frac{1}{\pi\sqrt{\pi R^{\mathrm{c}}}}\int_0^{2\pi}\int_0^{R^{\mathrm{c}}}\sqrt{R^{\mathrm{c}}2-\rho_0^2}\left\{\frac{\mathrm{e}^{-i\varphi}\tau(\rho_0,\ \varphi_0)}{R^{\mathrm{c}}2+\rho_0^2-2R^{\mathrm{c}}\cos(\varphi-\varphi_0)}\right.$$
$$\left.+\frac{\nu}{2-\nu}\frac{\mathrm{e}^{i\varphi}\{3R^{\mathrm{c}}-\rho_0\mathrm{e}^{i(\varphi-\varphi_0)}\}\bar{\tau}(\rho_0,\ \varphi_0)}{R^{\mathrm{c}}\{R^{\mathrm{c}}-\rho_0\mathrm{e}^{i(\varphi-\varphi_0)}\}^2}\right\}\rho_0\,\mathrm{d}\rho_0\,\mathrm{d}\varphi_0, \tag{A1}$$

where an overbar denotes a complex conjugate.

According to Gao (1988) and Kachanov and Laures (1989), we change from polar coordinate $(\rho_0,\ \varphi_0)$ in the crack plane to the new coordinate $(v,\ \zeta)$

$$v=\left[1+\frac{1}{d}\sqrt{R^{\mathrm{c}2}-\rho_0^2}\right]^{-1},\ \zeta=\sin^{-1}\left\{\frac{\rho_0}{d}\sin(\varphi_0-\varphi)\right\}, \tag{A2}$$

where $d^2=R^{\mathrm{c}}2+\rho_0^2-2R^{\mathrm{c}}\rho_0\cos(\varphi_0-\varphi)$ is the square of the distance between the point $(\rho_0,\ \varphi_0)$ and the point $(R^{\mathrm{c}},\ \varphi)$ along the crack front. Then Eq. (A1) is converted to the integral form:

$$K_1(\mathbf{z})=\frac{4\sqrt{\pi R^{\mathrm{c}}}}{\pi^2}\int_{-\pi/2}^{\pi/2}\int_0^1 p(v,\ \zeta)\frac{(1-v)^2\cos\zeta}{[(1-v)^2+v^2]^2}\,\mathrm{d}v\,\mathrm{d}\zeta,$$

$$K_2(\mathbf{z}) + iK_3(\mathbf{z}) = \frac{4\sqrt{\pi R^c}}{\pi^2} \int_{-\pi/2}^{\pi/2} \int_0^1 \frac{(1-\nu)^2 \cos\zeta}{[(1-\nu)^2+\nu^2]^2} \cdot \left\{ \tau e^{-i\varphi} + \frac{2\nu}{(2-\nu)} \bar{\tau} e^{i(\varphi-\zeta)} \times \left[e^{-i\zeta} + \frac{\nu^2 \cos\zeta}{(1-\nu)^2+\nu^2} \right] \right\} d\nu \, d\zeta, \tag{A3}$$

which are non-singulars. Here, we correct some misprints made in the papers by Kachanov and Laures (1989) and by Kachanov (1993) in Eqs. (A2) and (A3).

References

Arsenault, R.J., Taya, M., 1987. Thermal residual stress in metal matrix composite. Acta Metall. 35, 651–659.

Barnett, D.M., Asaro, R.J., 1972. The fracture mechanics of slit like cracks in anisotropic elastic media. J. Mech., Phys. Solids 20, 353–366.

Bensoussan, A., Lions, J.L., Papanicolaou, G., 1978. Asymptotic Analysis for Periodic Structures. North–Holland, Amsterdam, NY.

Bolotin, V.V. 1993. Random initial defects and fatigue life prediction. In: Sobczuk, K. (Ed.), Stochastic Approach to Fatigue: Experiments, Modeling and Reliability Estimation. Springer–Verlag, Wien, pp. 121–163.

Bover, A.F., Ortiz, W., 1993. The influence of grain size on the toughness of monolithic ceramic. J. Engng. Mater. Technol. 115, 228–236.

Budiansky, B., Hutchinson, J.W., Lambropoulos, J.C., 1983. Continuum theory of dilatant transformation toughening in ceramics. Int. J. Solids Structures 19, 337–355.

Buryachenko, V.A., 1996. The overall elastoplastic behavior of multiphase materials with isotropic components. Acta Mech. 119, 93–117.

Buryachenko, V.A., 1999a. Triply periodical particulate matrix composites in varying external stress fields. Int. J. Solids Structures 36, 3837–3859.

Buryachenko, V.A., 1999b. Internal residual stresses in elastically homogeneous solids: I. Statistically homogeneous stress fluctuations. Int. J. Solids Structures 37, 4185–4210.

Buryachenko, V.A., Kreher, W.S., 1995. Internal residual stresses in heterogeneous solids — A statistical theory for particulate composites. J. Mech. Phys. Solids 43, 1105–1125.

Buryachenko, V.A., Lipanov, A.M., 1986a. Stress concentration at ellipsoidal inclusions and effective thermoelastic properties of composite materials. Priklad. Mekh. 11, 105–111 (In Russian).

Buryachenko, V.A., Lipanov, A.M., 1986b. Stress concentration at ellipsoidal inclusions and effective thermoelastic properties of composite materials. Soviet Appl. Mech. 22 (11), 1103–1109 (English Translation).

Buryachenko, V.A., Parton, V.Z., 1990a. One-particle approximation of the effective field method in the statics of composites. Mekh. Kompoz. Mater. 3, 420–425 (In Russian).

Buryachenko, V.A., Parton, V.Z., 1990b. One-particle approximation of the effective field method in the statics of composites. Mech. Compos. Mater. 26 (3), 000–000 (English Translation).

Buryachenko, V.A., Parton, V.Z., 1992a. Effective field method in the statics of composites. Priklad. Mekh. Tekhn. Fiz. 5, 129–140 (In Russian).

Buryachenko, V.A., Parton, V.Z., 1992b. Effective field method in the statics of composites. J. Appl. Mech. Tech. Phys. 33, 735–745 (English Translation).

Buryachenko, V.A., Rammerstorfer, F.G., 1997. Elastic stress fluctuations in random structure particulate composites. Eur. J. Mechanics A/Solids 16, 79–102.

Buryachenko, V.A., Rammerstorfer, F.G., 1998. Thermoelastic stress fluctuations in random structure coated particulate composites. Eur. J. Mechanics A/Solids 17, 763–788.

Buryachenko, V.A., Rammerstorfer, F.G., 1999. On the thermostatics of composites with coated inclusions. Int. J. Solids Structures (in press).

Chudnovsky, A., Wu, S., 1993. Evaluation of energy release rate in the crack–microcrack interaction problem. Int. J., Solids Structure 29, 1699–1709.

Cutler, R.A., Vircar, A.V., 1985. The effect of binder thickness and residual stresses on the fracture toughness of cement carbide. J. Mater. Sci. 20, 3557–3573.

Evans, A.G., 1987. Microfracture from thermal expansion anisotropy; I. Single phase systems. Acta Metall. 26, 1845–1853.

Evans, A.G. 1989. The new high-toughness ceramics. In: Wei, R.P., Gangloff, R.P. (Eds.), Fracture Mechanics: Perspectives and Directions (Twentieth Symposium). Amer. Soc. Testing and Mater, pp. 267–291.
Fabrikant, V.I. 1989. Complete solutions to some mixed boundary value problems in elasticity. In: Hutchinson, J.W., Wu, T.J. (Eds.), Advances in Applied Mechanics. Acad. Press Inc, Boston, pp. 153–223.
Fu, Y., Evans, A.G., 1985. Some effects of microcracks on the mechanical properties of brittle solids; I. Stress–strain relation. Acta Metall. 33, 1515–1523.
Gao, H., 1988. Nearly circular shear mode cracks. Int. J. Solids, Structures 4, 177–193.
Jang, Z.G., Tennysin, R.C., 1989. Closure of cubic tensor polynomial failure surface. J. Comp. Mech. 23, 208–231.
Kachanov, M. 1993. Elastic solids with many cracks and related problems. In: Hutchinson, J., Wu, T. (Eds.), Advances in Applied Mechanics. Academic Press, NY, pp. 259–445.
Kachanov, M., Laures, J.-P., 1989. Three-dimensional problem of strongly interacting arbitrarily located penny-shaped cracks. Int. J. Fracture. 41, 289–313.
Lambropoulos, J.C., 1986. Spear, shape and orientation effects in transformation toughening. Int. J. Solids Structures 22, 1083–1106.
Laws, N., Lee, J.C., 1989. Microcracking in polycrystalline ceramics: elastic isotropy and thermal anisotropy. J. Mech. Phys. Solids 37, 603–618.
Lipetzky, P., Kreher, W., 1994. Statistical analysis of crack advance in ceramic composites. Mech. Mater. 20, 225–240.
Luo, J., Stevens, R., 1993. Residual stress and microcracking in Sic–MgO composites. J. European Ceramic Soc. 12, 369–375.
Ma, Q., Clarke, D.R., 1994. Piezospectroscopic determination of residual stresses in polycrystalline alumina. J. Amer. Ceram. Soc. 77, 298–302.
McMeeking, R.M., Evans, A.C., 1982. Mechanics of transformation toughening in brittle materials. J. Amer. Ceram. Soc. 69, 242–246.
Murakami, Y., 1987. Stress Intensity Factors Handbook, vol. 2. Pergamon Press, Oxford.
Nakamura, T., Suresh, S., 1993. Effects of thermal residual stresses and fiber packing on deformation of metal–matrix composites–sites. Acta Metall. Mater. 41, 1665–1681.
Nemat-Nasser, S., Hori, M., 1993. Micromechanics: Overall Properties of Heterogeneous Materials. Elsevier, Amsterdam.
Ortiz, M., Molinari, A., 1988. Microstructural thermal stresses in ceramic materials. J. Mech. Phys. Solids 36, 385–400.
Ortiz, M., Suresh, S., 1993. Statistical properties of residual stresses and intergranular fracture in ceramic materials. J. Appl. Mech. 60, 77–84.
Reifsnider, K.L., Gao, Z., 1991. A micromechanics models for composites under fatigue loading. Int. J. Fatigue. 13, 149–156.
Rice, J.R., 1985. Three-dimensional elastic crack tip interaction with transformation strains and dislocations. Int. J. Solids Structures 21, 781–791.
Rice, J.R. 1989. Weight function theory for three-dimensional elastic crack analysis. In: Wei, R.P., Gangloff, R.P. (Eds.), Fracture Mechanics: Perspectives and Directions (Twentieth Symp.). Amer. Soc. Test. and Mater, Philadelphia, pp. 29–57.
Rice, R.W., Pohanka, R.C., 1979. The grain size dependence of spontaneous-cracking in ceramics. J. Amer. Ceram. Soc. 62, 559–563.
Sobczuk, K., Spencer, B.F., 1991. Random Fatigue: From Data to Theory. Academic Press, NY.
Stump, D.M., Budiansky, B., 1989. Crack-growth resistance in transformation-toughened ceramics. Int. J. Solids Structures 25, 635–646.
Taya, M., Hayashi, S., Kobayashi, A.S., Yoon, H.S., 1990. Toughening of a particulate-reinforced ceramic–matrix composite by thermal residual stress. J. Amer. Ceram. Soc. 73, 1382–1391.
Theocaris, P.S., 1991. The elliptic paraboloid failure criterion for cellular solids and brittle forms. Acta Mechanica. 89, 93–121.
Tvergard, V., Hutchinson, J.W., 1988. Microcracking in ceramics by thermal expansion or elastic anisotropy. J. Amer. Ceram. Soc. 71, 157–166.
Walker, K.P., Jordan, E.H., Freed, A.D. 1990. Equivalence of Green's function and the Fourier series representation of composites with periodic microstructure. In: Weng, G.J., Taya, M., Abe, H. (Eds.), Micromechanics and Inhomogeneity. Springer–Verlag, NY, pp. 535–558.
Wang, B., 1990. A general theory of media with randomly distributed inclusions: I — The average field behaviors. J. Appl. Mech. 57, 857–862.
Wilson, W.K., Yu, L.W., 1979. The use of the *J*-integral in thermal stress crack problems. Int. J. Fracture 15, 377–387.